https://doi.org/10.5194/acp-2019-1132
Preprint. Discussion started: 6 January 2020

Atmospheric Chemistry and Physics Discussions

Predictions of the glass transition temperature and viscosity of organic aerosols by volatility distributions

Ying Li[1,*], Douglas A. Day[2,3], Harald Stark[2,3,4], Jose L. Jimenez[2,3] and Manabu Shiraiwa[1,*]

[1] Department of Chemistry, University of California, Irvine, CA 92697-2025, USA
[2] Cooperative Institute for Research in Environmental Sciences (CIRES), University of Colorado, Boulder, CO 80309, USA
[3] Department of Chemistry, University of Colorado, Boulder, CO 80309, USA
[4] Aerodyne Research Inc., Billerica, Massachusetts 01821, USA

*Correspondence to: Ying Li (yingl47@uci.edu) or Manabu Shiraiwa (m.shiraiwa@uci.edu)

https://doi.org/10.5194/acp-2019-1132
Preprint. Discussion started: 6 January 2020

Atmospheric Chemistry and Physics Discussions

Abstract:

Volatility and viscosity are important properties of organic aerosols (OA), affecting aerosol processes such as formation, evolution and partitioning of OA. Volatility distributions of ambient OA particles have often been measured, while viscosity measurements are scarce. We have previously developed a method to estimate the glass transition temperature (T_g) of an organic compound containing carbon, hydrogen, and oxygen. Based on analysis of over 2300 organic compounds including oxygenated organic compounds as well as nitrogen- and sulfur-containing organic compounds, we extend this method to include nitrogen- and sulfur-containing compounds based on elemental composition. In addition, parameterizations are developed to predict T_g as a function of volatility and the atomic oxygen-to-carbon ratio based on a negative correlation between T_g and volatility. The prediction method of T_g and viscosity is applied to ambient observations of volatility distributions at eleven field sites. The predicted T_g varies mainly from 290 K to 339 K and the predicted viscosities are consistent with the results of ambient particle phase state measurements in the southeastern US and the Amazonian rain forest. Reducing the uncertainties in measured volatility distributions would be helpful to improve predictions of viscosity especially at low relative humidity. We also predict the T_g of OA components identified via positive matrix factorization of aerosol mass spectrometer data. The predicted viscosity of oxidized OA is consistent with previously reported viscosity of SOA derived from α-pinene, toluene, isoprene epoxydiol (IEPOX), and of diesel fuel. Comparison of the predicted viscosity based on the observed volatility distributions with the viscosity simulated by a chemical transport model implies that missing low volatility compounds in a global model can lead to underestimation of OA viscosity at some sites. The relation between volatility and viscosity can be applied in the molecular corridor or volatility basis set approaches to improve OA simulations in chemical transport models by consideration of effects of particle viscosity in OA formation and evolution.

https://doi.org/10.5194/acp-2019-1132
Preprint. Discussion started: 6 January 2020

Atmospheric Chemistry and Physics Discussions

1. Introduction

Organic aerosols (OA) contribute substantially to the mass loadings of atmospheric fine particulate matter (Hallquist et al., 2009; Jimenez et al., 2009). OA formed from various anthropogenic or biogenic precursors have complex physicochemical properties (Goldstein and Galbally, 2007; Nizkorodov et al., 2011; Ditto et al., 2018), which makes predictions of their role in air quality, climate and public health challenging (Kanakidou et al., 2005; Shrivastava et al., 2017). Volatility and viscosity are important properties of OA, both of which affect important aerosol processes such as gas–particle partitioning, new particle formation and evolution of size distribution, heterogeneous reactions, and cloud condensation and ice nucleation pathways of OA, as summarized in recent review articles (Krieger et al., 2012; Bilde et al., 2015; Poschl and Shiraiwa, 2015; Knopf et al., 2018; Reid et al., 2018).

Recent measurements show that OA can exist in liquid (low dynamic viscosity η; $\eta < 10^2$ Pa s), semi-solid ($10^2 \leq \eta \leq 10^{12}$ Pa s), and amorphous solid ($\eta > 10^{12}$ Pa s) states (Reid et al., 2018). Even though there are several particle bounce measurements to infer ambient OA phase state, there are limited ambient measurements of particle phase state or viscosity depending on temperature (T), relative humidity (RH), and particle composition (Virtanen et al., 2010; O'Brien et al., 2014; Bateman et al., 2016; Pajunoja et al., 2016; Bateman et al., 2017; Liu et al., 2017; Ditto et al., 2019; Slade et al., 2019). Viscosity can be directly converted to bulk diffusivity in organic molecules using the Stokes–Einstein equation, which has been shown to work well for organic molecules diffusing through low viscous materials (Price et al., 2016; Chenyakin et al., 2017). This relation is inapplicable for predicting the bulk diffusivity of water and small molecules and it may also underestimate the diffusivity of organic molecules in a highly viscous matrix, which can be corrected using a fractional Stokes-Einstein equation (Price et al., 2016; Evoy et al., 2019).

Chemical composition of OA is complex and molecular specificity is often unavailable, which makes viscosity predictions of ambient OA challenging (Bosse,

https://doi.org/10.5194/acp-2019-1132
Preprint. Discussion started: 6 January 2020

Atmospheric Chemistry and Physics Discussions

2005; Song et al., 2016b; Rovelli et al., 2019). Viscosity can be related to the glass transition temperature (T_g), at which phase transition between amorphous solid and semi-solid states occurs (Koop et al., 2011). Ambient temperature varies through 100 K throughout the troposphere, greatly influencing the viscosity of the mixture. When the ambient temperature is below T_g, an amorphous particle behaves as a solid, while a particle would be semi-solid or liquid when the ambient temperature is above T_g. OA particles contain a number of organic compounds and also a variable amount of liquid water depending on RH, which can act as a plasticizer to reduce T_g: these mixture effects can be estimated using the Gordon-Taylor relation (Mikhailov et al., 2009; Koop et al., 2011; Dette et al., 2014). In addition, ambient OA may often be internally mixed with inorganic species such as sulfate and nitrate, which would further lower T_g and viscosity if they are well-mixed in one phase; when the phase separation occurs, the inorganic-rich and organic-rich phases may undergo glass transition at different temperatures (Dette and Koop, 2015).

We have recently developed a set of semi-empirical parameterizations using molar mass (M) and atomic O:C ratio (Shiraiwa and Li et al., 2017) or elemental composition (DeRieux and Li et al., 2018) to predict T_g for compounds comprised of carbon, hydrogen, and oxygen (CHO compounds). These parameterizations have been applied to high-resolution mass spectrometry measurements to estimate viscosity of organic aerosols (DeRieux and Li et al., 2018; Schum et al., 2018; Ditto et al., 2019) and coupled into a thermodynamic model (Gervasi et al., 2019). Note that heteroatoms and the effects of molecular structure and functional groups on T_g are not considered in parameterizations of Shiraiwa and Li et al. (2017) and DeRieux and Li et al. (2018).

Viscosity of pure compounds has been found to be inversely correlated with vapor pressure (Thomas et al., 1979). The molecular corridor (Shiraiwa et al., 2014; Li et al., 2016) based analysis of hundreds of SOA components has shown that compounds with lower pure compound saturation mass concentration (C^0) have higher T_g (Shiraiwa et al., 2017). Rothfuss & Petters (2017) found that there is a similar trend between the

https://doi.org/10.5194/acp-2019-1132
Preprint. Discussion started: 6 January 2020

Atmospheric Chemistry and Physics Discussions

sensitivity of viscosity to functional group addition and the sensitivity of vapor pressure to functional group addition. Measurements of the evaporation kinetics of maleic acid showed that decreasing particle viscosity leads to a suppression in the effective vapor pressure of maleic acid (Marshall et al., 2018). Champion et al. (2019) found secondary organic aerosols (SOA) with higher condensed-phase fractions of extremely low (ELVOC) and low volatile organic compounds (LVOC) showed an increased viscosity. Zhang et al. (2019) measured T_g of isoprene SOA components including isoprene hydroxy hydroperoxide (ISOPOOH), isoprene-derived epoxydiols (IEPOX), 2-methyltetrols, and 2-methyltetrol sulfates (2-MT-OS), observing a tight correlation between T_g and vapor pressure.

Based on the above evidence showing a close relation between volatility and viscosity, in this study we develop the parameterizations predicting T_g as a function of C^0 based on data from over 2000 compounds. Functional group contribution approaches are often used to predict C^0 (Capouet and Müller, 2006; Pankow and Asher, 2008; Compernolle et al., 2011; O'Meara et al., 2014), thereby using volatility to predict T_g would include the molecular structure effect indirectly. The developed parameterizations are applied to field observations of volatility distributions to predict viscosity of ambient OA.

2. Parameterizations

Figure 1a shows a dependence of T_g on C^0 of 2325 organic compounds compiled in previous studies with available measured otherwise estimated T_g and C^0 (Koop et al., 2011; Li et al., 2016; Rothfuss and Petters, 2017; Lessmeier et al., 2018). In this study "estimated T_g" represents the T_g estimated from the melting temperature (T_m) applying the Boyer-Kauzmann rule of $T_g = g \cdot T_m$ with $g = 0.7$ as validated in a previous study (Koop et al., 2011). The 2325 compounds are classified into four classes based on chemical composition: CH, CHO, CHON, and CHOS, with the number of 433, 783, 274, and 835, respectively. Detailed information of this dataset is described

https://doi.org/10.5194/acp-2019-1132
Preprint. Discussion started: 6 January 2020

Atmospheric Chemistry and Physics Discussions

in the Supplement. Figure 1a shows compounds with lower C^0 have higher T_g and the T_g appears to level at around 420 K at $C^0 < \sim 10^{-10}$ μg m^{-3}. The dependence of T_g on the atomic O:C ratio is weaker (Fig. 1a), in agreement with previous studies (Koop et al., 2011; Shiraiwa et al., 2017). Based on the trend shown in Fig. 1a, we develop a parameterization (Eq. 1) to predict T_g as a function of C^0 and the atomic O:C ratio, which are the parameters used in the two-dimensional VBS (2D-VBS) framework (Donahue et al., 2011):

$$T_g = 289.10 - 16.50 \times \log_{10}(C^0) - 0.29 \times [\log_{10}(C^0)]^2 + 3.23 \times \log_{10}(C^0)\ (\text{O:C}) \quad (1)$$

The coefficients in Eq. (1) are obtained by fitting the T_g of 2325 compounds in Fig. 1a with multi-linear least squares analysis with 68% prediction and confidence intervals. Figure 1b shows that the T_g of those 2325 compounds are predicted well by Eq. (1) as indicated by a high correlation coefficient (R) of 0.92. The average absolute value of the relative error (AAVRE, Aiken et al., 2007) is 12%. T_g of individual compounds can be predicted within ±31 K as indicated by the prediction band (dotted lines in Fig. 1b); however, this uncertainty may be much smaller for multicomponent SOA mixtures under ideal mixing conditions as indicated in the confidence band (dashed lines, almost overlapping with the 1:1 line) (Shiraiwa and Li et al., 2017; DeRieux and Li et al., 2018; Song et al., 2019).

Equation (1) is also evaluated with a different set of organic compounds as a test dataset, including 654 CHO compounds and 212 CHON compounds found in SOA oxidation products (Shiraiwa et al., 2014). The values of their T_g are predicted by Eq. (1) with saturation mass concentrations estimated using the EVAPORATION model (Compernolle et al., 2011). The predicted T_g by Eq. (1) are compared with the T_g estimated from the T_m applying the Boyer-Kauzmann rule. T_m values are adopted from the estimations of the Estimation Programs Interface (EPI) Suite software (version 4.1) developed by the US Environmental Protection Agency (US EPA, 2015). As shown in

https://doi.org/10.5194/acp-2019-1132
Preprint. Discussion started: 6 January 2020

Atmospheric Chemistry and Physics Discussions

Fig. 1(c), Eq. (1) also presents a good performance for predicting the T_g of these SOA components with R = 0.96 and AAVRE = 6 %. Note that Eq. (1) was developed based on the training dataset containing a large number of compounds with measured C^0 (Table S1 in Supplement) and aimed to be applied in the 2D-VBS framework to predict the viscosity of SOA mixtures. For pure organic compounds with known molecular structure, viscosity can be predicted by group contribution approaches (Cao et al., 1993; Bosse, 2005; Song et al., 2016b; Gervasi et al., 2019; Rovelli et al., 2019).

We also develop a parameterization (Eq. 2) predicting T_g as a function of C^0 solely, which could be applied to the information available with the one-dimensional VBS (1D-VBS) framework (Donahue et al., 2006), and can be used when the O:C ratio is not available in measurements.

$$T_g = 288.70 - 15.33 \times \log_{10}(C^0) - 0.33 \times [\log_{10}(C^0)]^2 \quad (2)$$

The coefficients in Eq. (2) are obtained following the procedures developing Eq. (1) and the same training dataset is used. Figure S1 shows that Eq. (2) gives very similar predictions as Eq. (1) particularly for the compounds with low O:C ratio. As Eq. (1) and (2) are developed based on the compounds with their C^0 higher than ~10^{-20} μg m^{-3}, Eqs. (1–2) may not be applicable for compounds with C^0 < ~10^{-20} μg m^{-3} (Fig. 1a).

We recently developed a parameterization (Eq. 3) predicting T_g as a function of the number of carbon (n_C), hydrogen (n_H), and oxygen (n_O) atoms (DeRieux and Li et al., 2018), similar to the formulation used to predict C^0 (Donahue et al., 2011; Li et al., 2016).

$$T_g = (n_C^0 + \ln(n_C))\, b_C + \ln(n_H)\, b_H + \ln(n_C) \ln(n_H)\, b_{CH} + \ln(n_O)\, b_O + \ln(n_C) \ln(n_O)\, b_{CO} \quad (3)$$

Values of the coefficients [n_C^0, b_C, b_H, b_{CH}, b_O, and b_{CO}] are [1.96, 61.99, -113.33, 28.74, 0, 0] for CH compounds and [12.13, 10.95, -41.82, 21.61, 118.96, -24.38] for CHO

https://doi.org/10.5194/acp-2019-1132
Preprint. Discussion started: 6 January 2020

Atmospheric Chemistry and Physics Discussions

compounds. We broaden the parameterizations for CH and CHO compounds (Eq. 3) to the following equations applicable to CHON (Eq. 4) and CHOS compounds (Eq. 5):

$$T_g = (n_C^0 + \ln(n_C))\, b_C + \ln(n_O)\, b_O + \ln(n_N)\, b_N + \ln(n_C) \ln(n_O)\, b_{CO} + \ln(n_C) \ln(n_N)\, b_{CN} + \ln(n_O) \ln(n_N)\, b_{ON} \quad (4)$$

$$T_g = (n_C^0 + \ln(n_C))\, b_C + \ln(n_O)\, b_O + \ln(n_S)\, b_S + \ln(n_C) \ln(n_O)\, b_{CO} + \ln(n_C) \ln(n_S)\, b_{CS} + \ln(n_O) \ln(n_S)\, b_{OS} \quad (5)$$

Values of the coefficients [n_C^0, b_C, b_O, b_N, b_{CO}, b_{CN} and b_{ON}] in Eq. (4) are [5.34, 31.53, -7.06, 134.96, 6.54, -34.36, -15.35] and [n_C^0, b_C, b_O, b_S, b_{CO}, b_{CS} and b_{OS}] in Eq. (5) are [1.12, 68.41, 64.95, 35.77, -12.32, -9.85, 13.80], respectively. These values are obtained by fitting the T_g of CHON and CHOS compounds included in the training dataset (Fig. 1a, Table S1) with multi-linear least squares analysis. In the training dataset there are 35 CHON compounds with measured T_g available (Koop et al., 2011) and T_g of other 239 CHON compounds are estimated by the Boyer-Kauzmann rule using their measured T_m (Supplement). Figure 2(a) shows a fair agreement between the predicted T_g using Eq. (4) and the measured otherwise estimated T_g with R of 0.55 and relatively large AAVRE of 16 %. Figure 2 (b) shows a better prediction performance with R of 0.83 and AAVRE of 9 % for 212 CHON compounds included in the test dataset with estimated T_g by the Boyer-Kauzmann rule using the EPI-estimated T_m. Measured T_g values for CHOS compounds are sparse (Zhang et al., 2019) and the T_g of the 835 CHOS compounds shown in Fig. 2c are estimated by the Boyer-Kauzmann rule using the EPI-estimated T_m. Figure 2 (c) shows that Eq. 5 performs well for those CHOS compounds with R of 0.87 and AAVRE of 8 %.

Comparison of T_g predicted by Eqs. (4, 5) with T_g predicted by Eq. (1) shows that the agreement between the two sets of parameterizations for nitrogen- and sulfur-containing compounds is not as good as that for CHO compounds (Fig. S2), indicating that there are limitations of predicting T_g by the elemental composition for nitrogen-

https://doi.org/10.5194/acp-2019-1132
Preprint. Discussion started: 6 January 2020

Atmospheric Chemistry and Physics Discussions

and sulfur-containing compounds with complex elemental composition and molecular structures. As volatility depends significantly on functional groups contained in a molecule (Pankow and Asher, 2008; Compernolle et al., 2011), predicting T_g by volatility (Eq. 1) indirectly incorporates the effects of molecular structure. Considering Eqs. (4, 5) are useful in high-resolution mass spectrometry measurements (DeRieux and Li et al., 2018; Schum et al., 2018), future experiments measuring more T_g data for nitrogen- and sulfur-containing organics would help improve the T_g parameterizations.

Recently Zhang et al. (2019) developed a semi-empirical parameterization (Eq. 6) using vapor pressure (p_0 in atm) to predict T_g based on measured T_g of 11 SOA compounds:

$$T_g = 480.1 - \frac{54395}{(log_{10}(p_0)-1.7929)^2+116.49} \quad (6)$$

p_0 can be converted to C^0 via $C^0 = (10^6 M\, p_0)/(RT)$, where R is the ideal gas constant (R = 8.2 ×10^{-5} m^3 atm mol^{-1} K^{-1}), M is the molar mass (g mol^{-1}), and T is the temperature (K). Figure 3 compares the measured T_g (Koop et al., 2011; Rothfuss and Petters, 2017; Lessmeier et al., 2018; Zhang et al., 2019) to T_g predicted by (a) C^0 and the atomic O:C (Eq. 1), (b) elemental composition (Eqs. 3-5), and (c) Eq. (6) by Zhang et al. (2019). While all three methods perform reasonably well, the predictions using elemental composition (Eqs. 3-5) show better performance (Fig. 3b) with R of 0.93 and AAVRE of 11 %, respectively.

The prediction performance is influenced by the training dataset used developing parameterizations of T_g. The compounds shown in Fig. 3 contain mostly carboxylic acid and hydroxyl functional groups (Koop et al., 2011; Rothfuss and Petters, 2017) and are included in the training dataset used developing Eq. (1) and Eqs. (3-5). The training dataset used in Zhang et al. (2019) included 11 organic compounds, and their parameterization predicted T_g of isoprene SOA very well (Zhang et al., 2019), while underpredicting some low-T_g compounds (Fig. 3c). For compounds with their

https://doi.org/10.5194/acp-2019-1132
Preprint. Discussion started: 6 January 2020

measured T_g higher than 200 K, predictions by Zhang et al. (2019) show good performance and are consistent with the predictions given by Eq. (1). Predicted T_g of 2-MT-OS using the three methods are 297 K (Eq. 1), 275 K (Eq. 5) and 280 K (Eq. 6), comparable with the measured T_g of 276 ± 15 K (Zhang et al., 2019).

Note that predictions using elemental composition (Eq. 3) overestimate the T_g of phthalate compounds (the star markers in Fig. 3). For instance, the observed T_g of dioctyl phthalate is 194 K (Zhang et al., 2018), while the prediction is higher than 300 K (Fig. 3b). The reason is that ester is not an effective functional group to increase viscosity compared to carboxylic acid and hydroxyl (Rothfuss and Petters, 2017). Parameterizations using volatility (Eqs. 1 and 6) improve the predicted T_g of phthalate compounds (Fig. 3a, c). Figure A1 shows comparing to the predictions using Eq. (6) provided in Zhang et al. (2019), predictions by C^0 and the atomic O:C (Eq. 1) and elemental composition (Eq. 3) agree better with the T_g estimated from the Boyer-Kauzmann rule. Future experiments measuring more T_g of SOA components would help verify the T_g predictions by different parameterizations.

3. Application in field observations

T_g of ambient OA are estimated by applying the developed parameterizations to field observations of volatility distributions. The term volatility refers to the effective saturation mass concentration (C^*) and we assume ideal thermodynamic mixing in which case C^* is equal to C^0 (Donahue et al., 2011). T_g are then placed into the 2D-VBS framework of O:C ratio vs. volatility as shown in Fig. 4. The isolines in Fig. 4 show the predicted T_g by Eq. (1), showing that T_g would be below ~ 250 K for intermediate volatility organic compounds (IVOC; $300 < C^0 < 3\times10^6$ μg m^{-3}), from ~ 260 K to 290 K for semi-volatile organic compounds (SVOC; $0.3 < C^0 < 300$ μg m^{-3}), and higher than 300 K for low-volatile organic compounds (LVOC; $3\times10^{-4} < C^0 < 0.3$ μg m^{-3}) and extremely low-volatile organic compounds (ELVOC; $C^0 < 3\times10^{-4}$ μg m^{-3}). T_g increases as the O:C ratio increases for SVOC and IVOC, consistent with previous studies (Koop

https://doi.org/10.5194/acp-2019-1132
Preprint. Discussion started: 6 January 2020

et al., 2011; Saukko et al., 2012; Berkemeier et al., 2014). T_g slightly decreases as the O:C ratio increases for LVOC and ELVOC compounds, which might be due to the uncertainties in Eq. (1) which is derived from a dataset containing fewer LVOC and ELVOC compounds as shown in Fig. 1a, which exhibits lower T_g with higher O:C.

3.1 Southern Oxidant and Aerosol Study (SOAS)

The volatility of ambient OA was measured during the SOAS campaign which took place in the southeastern United States (Centreville, Alabama) in summer 2013 (Carlton et al., 2018). T_g in each volatility bin ($T_{g,i}$) is calculated by Eq. (1) under the assumption of ideal thermodynamic mixing and the measured O:C is used (Xu et al., 2015). The glass transition temperatures of organic aerosols under dry conditions ($T_{g,org}$) are calculated by the Gordon-Taylor equation assuming the Gordon-Taylor constant (k_{GT}) of 1: $T_{g,org} = \sum_i w_i T_{g,i}$ (Dette et al., 2014) , where w_i is the mass fraction in the particle phase for each volatility bin (Table S2). To place $T_{g,org}$ into the 2D-VBS framework, the average $\log_{10}(C^*)$ is calculated by $\sum_i w_i log_{10}(C_i^*)$ (Kostenidou et al., 2018).

Figure 4 shows that $T_{g,org}$ of total OA (TOA) ranges from 232 K to 334 K, depending on volatility distributions measured by different methods. Stark et al. (2017) used three methods to derive volatility distributions applying the measurements of organic acids (which comprised half of the total OA; Yatavelli et al., 2015) from a high-resolution chemical ionization time-of-flight mass spectrometer (HRToF-CIMS) equipped with a filter inlet for gases and aerosols (FIGAERO, Lopez-Hilfiker et al., 2014; Thomson et al., 2017). The "Formulas" method used the SIMPOL group contribution method (Pankow and Asher, 2008) to calculate vapor pressures from the composition of the identified ions. Many of the detected species can be thermal decomposition products rather than actual SOA molecules (Stark et al., 2015; Stark et al., 2017), which can lead to overestimations of volatilities mainly in the IVOC range, resulting in the unlikely low $T_{g,org}$ of 232 K. The "Partitioning" method used the

https://doi.org/10.5194/acp-2019-1132
Preprint. Discussion started: 6 January 2020

Atmospheric Chemistry and Physics Discussions

measured particle-phase mass fractions of each species to estimate C^* based on the partitioning theory (Pankow, 1994). The estimated C^* is distributed mainly in the SVOC range (Stark et al., 2017), leading to a $T_{g,org}$ of 279 K (Fig. 4). This value is very close to the $T_{g,org}$ (281 K) simulated by a global chemical transport model EMAC-ORACLE (Shiraiwa et al., 2017). However, Stark et al. (2017) note that the partitioning-based volatility distribution is likely too high due to an artifact of signal-to-noise limitations, confining the C^* characterizable by the partitioning method to a relatively narrow range centered around the ambient OA concentration (by definition, the semi-volatile range). In the thermogram method, C^* at 298 K is estimated from the desorption temperature after calibration with known species (Faulhaber et al., 2009). This method results in 93% of OA mass distributed in the LVOC and ELVOC (Stark et al., 2017), and a high $T_{g,org}$ of 330 K is predicted (Fig. 4). These analyses indicate that the volatility distributions derived from different methods, even when based on the same measurements, significantly affect the predicted $T_{g,org}$.

Among these three methods using CIMS measurements of organic acids, Stark et al. (2017) note that the result from the thermogram method is more consistent with those measured by an aerosol mass spectrometer (AMS) with a thermo denuder (TD), which also applied the thermogram method to estimate the C^* distributions (Hu et al., 2016). Saha et al. (2017) applied an evaporation kinetic model (Lee et al., 2011) based on the VBS approach to extract the C^* distributions, and the effects of enthalpy of vaporization (ΔH_{vap}) and accommodation coefficient (α) are considered, resulting in the estimated $T_{g,org}$ of 313 K. This study retrieved α ~0.5, which is consistent with recent observations (Krechmer et al., 2017; Liu et al., 2019). In summary, $T_{g,org}$ during the SOAS campaign span the range of 313 – 330 K.

Figure 4 also shows $T_{g,org}$ of OA components identified via positive matrix factorization (PMF) of the aerosol mass spectrometer data. Isoprene-epoxydiols-derived SOA (IEPOX-SOA) has $T_{g,org}$ of 345 K with very low volatility with the average C^* lower than 10^{-4} μg m^{-3} (Hu et al., 2016; Lopez-Hilfiker et al., 2016; D'Ambro

https://doi.org/10.5194/acp-2019-1132
Preprint. Discussion started: 6 January 2020

Atmospheric Chemistry and Physics Discussions

et al., 2019), which may be due to substantial formation of organosulfates and other oligomers (Lin et al., 2012; Hu et al., 2015; Riva et al., 2019).The predicted $T_{g,org}$ of IEPOX-SOA is higher than previously reported $T_{g,org}$ of 263 - 293 K for monoterpene-derived (α-pinene, Δ^3-carene, myrcene, limonene and ocimene) SOA (Petters et al., 2019).

The phase state of aerosol particles strongly depends on their water content (Mikhailov et al., 2009; Koop et al., 2011). Under humid conditions, T_g of organic-water mixtures at given RH can be estimated considering hygroscopic growth combined with the Gordon-Taylor equation. The effective hygroscopicity parameter (κ) (Petters and Kreidenweis, 2007) of TOA during the SOAS is measured as 0.14 (Cerully et al., 2015). The Gordon-Taylor constant for organic-water mixtures is suggested to be 2.5 (Zobrist et al., 2008; Koop et al., 2011). Using the T_g of organic-water mixtures, the temperature-dependence of viscosity can be calculated applying the Vogel-Tammann-Fulcher (VTF) equation (Angell, 1991; Rothfuss and Petters, 2017; DeRieux and Li et al., 2018). Figure 5(a) shows the predicted viscosity of total OA at different RH. T is adopted as 298 K, the average value during the SOAS campaign (Hu et al., 2016). The characteristic timescale of mass transport and mixing by molecular diffusion (τ_{mix}) is also calculated: $\tau_{mix} = d_p^2 / (4\pi^2 D_b)$ (Seinfeld and Pandis, 2006), where d_p is the particle diameter and the bulk diffusion coefficient D_b is calculated from the predicted viscosity by the fractional Stokes–Einstein relation (Evoy et al., 2019). We assume the radius of the diffusing molecule of 10^{-10} m and the particle diameter of 200 nm (Shiraiwa et al., 2011). Note that these estimated timescales represent rough estimations, as molecular interactions in complex mixtures are not considered.

The viscosity of TOA at RH of 83% (average RH during SOAS) is predicted to be less than 10^2 Pa s with τ_{mix} less than 1 s, which is consistent with the particle bounce measurements which suggested organic-dominated particles were mostly liquid during the SOAS campaign (Pajunoja et al., 2016). When RH was below ~50% in the sampling inlet, the particles were found to adopt a semi-solid state (Pajunoja et al.,

https://doi.org/10.5194/acp-2019-1132
Preprint. Discussion started: 6 January 2020

2016), which agrees with the predicted viscosity of $10^7 – 10^{11}$ Pa s and τ_{mix} can be higher than 1 hour at RH of 50% (Fig. 5a).

Figure 5(b) shows diurnal variations of predicted viscosity of total OA using measured T and RH during the SOAS campaign (Hu et al., 2016). During 10:00 – 20:00 when RH < 70 % and T > 298 K, three simulations using different $T_{g,org}$ values predict that total OA occur as semi-solid with the predicted viscosity of $10^2 – 10^7$ Pa s and the mixing times less than 1 hour. Particles are predicted to have low viscosity of < 1 Pa s adopting a liquid phase during nighttime. The lowest viscosity occurs around 5:00 – 6:00 with RH > 95 %. Here we did not consider the effects of the diurnal variations of volatility distributions, as they did not vary dramatically over the campaign period (Saha et al., 2017). Besides T and RH, diurnal variation of ambient aerosol phase state also depends on particle chemical composition and mixing states. Organic particles in Amazon were found to be more viscous at night than the daytime due to the influence of biomass burning that may form non-liquid particles (Bateman et al., 2017). Particles in a mixed forest in northern Michigan were also found more viscous at night despite higher RH than the daytime, due to the formation of high molar mass organic compounds and smaller inorganic sulfate mass fractions (Slade et al., 2019). Phase state measurements during daytime and nighttime at Atlanta suggested that the ambient particle phase state was influenced by OA composition, the presence of inorganic ions, aerosol liquid water and particle mixing state (Ditto et al., 2019).

3.2 $T_{g,org}$ at 11 global sites

Figure 6 summarizes $T_{g,org}$ at 11 sites where the measured volatility distributions with volatility bins of four or more are available (Table S2). We did not include the data with narrower volatility ranges which may not correctly characterize the properties of ambient SOA (Bilde et al., 2015), and thus may not be appropriate for estimating fundamental particle properties and volatility distributions without considering realistically low C^* bins would result in too low T_g. Note that a narrow VBS

https://doi.org/10.5194/acp-2019-1132
Preprint. Discussion started: 6 January 2020

Atmospheric Chemistry and Physics Discussions

may still be useful for efficiency in 3-dimentional chemical transport models for SOA evaporation and condensation under the narrow range of ambient temperature variations (Kostenidou et al., 2018). $T_{g,org}$ is color-coded in the 2D-VBS framework of O:C vs. $\log_{10}C^*$ in the panel (a), whereas the panel (b) shows $T_{g,org}$ vs. $\log_{10}C^*$ with markers color-coded with the O:C ratio. $T_{g,org}$ of total OA (TOA) varies from 290 K to 339 K. The lower $T_{g,org}$ occurs at Beijing, China in June 2018 (Xu et al., 2019). OA in Beijing was found to be overall more volatile with the particle-phase semi-volatile fraction of 63%, leading to a lower $T_{g,org}$. The predicted $T_{g,org}$ of total OA at numerous other sites range between 300 K and 320 K, including Paris (Paciga et al., 2016), Mexico city (Cappa and Jimenez, 2010), Centreville (Hu et al., 2016; Saha et al., 2017; Stark et al., 2017), Raleigh (Saha et al., 2017), and Durham (Saha et al., 2018) in southeastern US. The $T_{g,org}$ (316 K) is higher at 220 m from a highway in Durham than the $T_{g,org}$ (309 K) at 10 m downwind distance due to the dilution and mixing of traffic-sourced particles with background air and evaporation of semi-volatile species during downwind transport (Saha et al., 2018). $T_{g,org}$ is predicted to be higher (>320 K) at the sites in Athens, Pasadena, Colorado Rocky Mountain and Amazon (Fig. 6).

At the same site in Mexico city or Athens, Figure 6 shows that the $T_{g,org}$ is lowest for the BBOA factor (287 K – 305 K) followed by HOA (290 K – 331 K) and OOA (> 350 K for the MO-OOA in Mexico city and Paris), which follows the trend of the decrease in the average volatility of these OA factors. Cooking OA (COA) has comparable $T_{g,org}$ (290 K – 324 K) with HOA. Marine OA (MOA) was characterized with high volatility containing around 60% SVOC, leading to the $T_{g,org}$ of 295 K in summer in Paris.

Figure 7 shows the OA viscosity variation of OA components against RH. The hygroscopic growth is considered based on hygroscopicity (κ), which is estimated as a function of the O:C ratio (Lambe et al., 2011) when κ was not measured (Table S2). Figure 7a shows OA factors with low O:C ratio, i.e., HOA, COA and BBOA, occur as liquid only when RH is very high (> ~80 %), as their κ is estimated to be low (<

https://doi.org/10.5194/acp-2019-1132
Preprint. Discussion started: 6 January 2020

Atmospheric Chemistry and Physics Discussions

0.08). HOA, COA and BBOA in Athens and COA in Paris can undergo glass transition (i.e., viscosity reaches 10^{12} Pa s) at RH between 25 % and 68 %. OA factors with higher O:C ratio and hygroscopicity including LO-OOA, MO-OOA, IEPOX SOA and isoprene-OA tend to become liquid (viscosity < 10^2 Pa s) at intermediate RH (Fig. 7b).

The predicted ambient viscosity is compared with the experimental observed viscosity of SOA formed from isoprene (Song et al., 2015), α-pinene (Abramson et al., 2013; Renbaum-Wolff et al., 2013; Kidd et al., 2014; Pajunoja et al., 2014; Bateman et al., 2015; Zhang et al., 2015; Grayson et al., 2016; Petters et al., 2019), toluene (Song et al., 2016a) and diesel fuel (Song et al., 2019). The majority of experimental values are well bounded by the predicted viscosity of OOA, represented by the pink shaded area. One exception is the measured viscosity of isoprene SOA is lower than the predicted viscosity of IEPOX SOA at low RH (<30 %). One possible reason is that the isoprene SOA in experiments was formed with high oxidant concentrations with short reaction time in an oxidation flow reactor in the absence of inorganic seed particles (OFR) (Song et al., 2015). In ambient environments heterogeneous reactions with acidic sulfate particles forming oligomers are suggested to be an important pathway (Surratt et al., 2010; Lin et al., 2013; Hu et al., 2015, 2016). These particle-phase organosulfates may contribute to a higher viscosity, as indicated by the predicted viscosity of IEPOX-derived organosulfate mixtures with their $T_{g,org}$ estimated to be 313 K (Riva et al., 2019). Another reason could be the mass concentrations (100 ~ 1000 μg m^{-3}) of isoprene SOA generated in the OFR (Song et al., 2015) are much higher than the ambient OA concentrations (5 μg m^{-3}, Stark et al., 2017) observed during the SOAS campaign. Higher mass concentrations can lead to lower viscosity, as more semi-volatile compounds can partition into the particle phase (Pankow, 1994; Donahue et al., 2006; Grayson et al., 2016; Jain et al., 2018; Champion et al., 2019).

4. Implications on SOA simulations in chemical transport models

https://doi.org/10.5194/acp-2019-1132
Preprint. Discussion started: 6 January 2020

Atmospheric Chemistry and Physics Discussions

Shiraiwa et al. (2017) simulated the global distribution of annual averages of SOA phase state using the chemical transport model EMAC (Jöckel et al., 2006) coupled with the organic aerosol module ORACLE (Tsimpidi et al., 2014). ORACLE uses the 1D-VBS framework with four C^* bins (1, 10, 10^2, and 10^3 μg m^{-3}). To estimate T_g the values of molar mass and O:C ratio were assigned for each volatility bin based on molecular corridors (Shiraiwa et al., 2014). Note that the molar mass assigned for the volatility bin of 1 μg m^{-3} was assumed to have relatively high molar mass to partially compensate for the fact that ORACLE does not consider lower volatility bins with higher molar mass. Global distributions of T_g /T presented in Shiraiwa et al. (2017) is converted to viscosity using the VTF equation, as shown in Fig. 8. Figure 8 also includes the viscosity of total OA at 11 sites by applying the model simulated 5 years' average T and RH with κ assumed to be 0.1 (Pringle et al., 2010). It shows the predicted viscosity at 11 sites (markers) generally agree well with the global simulations: the amorphous solid or semi-solid phase occurs over relatively dry lands, including western US, Mexico city, and Beijing; the lower viscosity occurs in southeastern US and Paris.

The global simulations show that the particles are liquid in the Amazon, while they occur as semi-solid in our predictions based on measured volatility distributions. The reason of this disagreement may be mainly due to the substantial fraction of low volatility compounds observed in ambient measurements largely missing from global simulations. Hu et al. (2016) observed that 90% of OA have volatilities lower than 1 μg m^{-3}, which is the lowest C^* bin in the global simulations. The ambient phase state measurements show that for background conditions of the Amazonian tropical forest, particles are mostly liquid, while with the anthropogenic influence of biomass burning, they occur as a nonliquid phase (Bateman et al., 2016; Bateman et al., 2017). The volatility distributions were measured in the dry season heavily influenced by biomass burning (Hu et al., 2016), which can lead to the higher predicted viscosity. A similar case is observed in Athens, that our predictions indicate

https://doi.org/10.5194/acp-2019-1132
Preprint. Discussion started: 6 January 2020

464 the glassy phase state while the global model predicts the occurrence of a semi-solid
465 phase.

466 Most of the current chemical transport models treat particles as liquid or
467 homogeneously well-mixed without considering particle-phase diffusion limitations
468 (Pankow, 1994), which can lead to bias in simulations of SOA mass concentrations and
469 evolution of size distributions (Shiraiwa and Seinfeld, 2012; Zaveri et al., 2018). The
470 SOA simulations applying the VBS framework have not included the effects of
471 viscosity on SOA formation and evolution. When the gas-particle partitioning is in the
472 bulk diffusion-limited regime, kinetic treatments of SOA partitioning may need to be
473 applied (Perraud et al., 2012; Liu et al., 2016; Yli-Juuti et al., 2017; Li and Shiraiwa,
474 2019). Some chamber experiments probing the mixing timescales of SOA particles did
475 not observe significant kinetic limitations at moderate and high RH under room
476 temperature (Loza et al., 2013; Ye et al., 2018), warranting further investigations on the
477 degree of kinetic limitations in ambient tropospheric conditions. The method developed
478 in this study can be applied in the VBS or the molecular corridor-based approach to
479 improve OA simulations in chemical transport models (Pye et al., 2017; Schmedding
480 et al., 2019). Several important aspects should be further explored in future studies. The
481 interplay of diffusion limitations and phase separation impacts heterogeneous and
482 multiphase chemistry (Vander Wall et al., 2018; DeRieux et al., 2019; Zhou et al., 2019)
483 and gas-particle partitioning (Zuend and Seinfeld, 2012; Freedman, 2017; Pye et al.,
484 2017; Gorkowski et al., 2019a). The particle morphology and the degree of non-ideal
485 mixing and liquid-liquid phase separation can evolve upon atmospheric aging
486 (Gorkowski et al., 2019b). These aspects may also need to be considered for better
487 representation of organic aerosols in future studies.
488

489 **Author contribution.**

490 YL, JLJ and MS designed the research. YL developed the parameterizations. DAD, HS
491 and JLJ provided measured volatility distributions for the SOAS campaign. YL and MS

https://doi.org/10.5194/acp-2019-1132
Preprint. Discussion started: 6 January 2020

wrote the manuscript. All authors discussed the results and contributed to manuscript editing.

Data availability. The data used in this study is available in the supplement.

Competing interests. The authors declare that they have no conflict of interest.

Acknowledgements. This work was funded by the National Science Foundation (AGS-1654104) and the Department of Energy (DE-SC0018349). The CU-Boulder group was supported by DOE (BER/ASR) DE-SC0016559 and NSF AGS-1822664. We thank A. Tsimpidi, V. Karydis, S. Pandis and J. Lelieveld for global simulations of SOA concentrations used to calculate T_g/T (as presented in Shiraiwa et al., 2017), which are converted into viscosity (Fig. 8). We also thank Sergey Nizkorodov, Andreas Zuend, Yue Zhang, Jason Surratt and Markus Petters for stimulating discussions.

References:

Abramson, E., Imre, D., Beranek, J., Wilson, J. M. and Zelenyuk, A.: Experimental determination of chemical diffusion within secondary organic aerosol particles, Phys. Chem. Chem. Phys., 15, 2983-2991, https://doi.org/10.1039/c2cp44013j, 2013.

Aiken, A. C., DeCarlo, P. F. and Jimenez, J. L.: Elemental analysis of organic species with electron ionization high-resolution mass spectrometry, Anal. Chem., 79, 8350-8358, https://doi.org/10.1021/ac071150w, 2007.

Angell, C.: Relaxation in liquids, polymers and plastic crystals—strong/fragile patterns and problems, J. Non-Cryst. Solids, 131-133, 13-31, https://doi.org/10.1016/0022-3093(91)90266-9, 1991.

Bateman, A. P., Bertram, A. K. and Martin, S. T.: Hygroscopic influence on the semisolid-to-liquid transition of secondary organic materials, J. Phys. Chem. A, 119, 4386-4395, https://doi.org/10.1021/jp508521c, 2015.

Bateman, A. P., Gong, Z., Liu, P., Sato, B., Cirino, G., Zhang, Y., Artaxo, P., Bertram, A. K., Manzi, A. O., Rizzo, L. V., Souza, R. A. F., Zaveri, R. A. and Martin, S. T.: Sub-micrometre particulate matter is primarily in liquid form over Amazon rainforest, Nat. Geosci., 9, 34-37, https://doi.org/10.1038/ngeo2599, 2016.

https://doi.org/10.5194/acp-2019-1132
Preprint. Discussion started: 6 January 2020

525 Bateman, A. P., Gong, Z., Harder, T. H., de Sá, S. S., Wang, B., Castillo, P., China, S.,
526 Liu, Y., O'Brien, R. E., Palm, B. B., Shiu, H. W., Cirino, G. G., Thalman, R.,
527 Adachi, K., Alexander, M. L., Artaxo, P., Bertram, A. K., Buseck, P. R., Gilles,
528 M. K., Jimenez, J. L., Laskin, A., Manzi, A. O., Sedlacek, A., Souza, R. A. F.,
529 Wang, J., Zaveri, R. and Martin, S. T.: Anthropogenic influences on the physical
530 state of submicron particulate matter over a tropical forest, Atmos. Chem. Phys.,
531 17, 1759-1773, https://doi.org/10.5194/acp-17-1759-2017, 2017.
532 Berkemeier, T., Shiraiwa, M., Pöschl, U. and Koop, T.: Competition between water
533 uptake and ice nucleation by glassy organic aerosol particles, Atmos. Chem.
534 Phys., 14, 12513-12531, https://doi.org/10.5194/acp-14-12513-2014, 2014.
535 Bilde, M., Barsanti, K., Booth, M., Cappa, C. D., Donahue, N. M., Emanuelsson, E. U.,
536 McFiggans, G., Krieger, U. K., Marcolli, C., Topping, D., Ziemann, P., Barley,
537 M., Clegg, S., Dennis-Smither, B., Hallquist, M., Hallquist, Å. M., Khlystov,
538 A., Kulmala, M., Mogensen, D., Percival, C. J., Pope, F., Reid, J. P., Ribeiro da
539 Silva, M. A. V., Rosenoern, T., Salo, K., Soonsin, V. P., Yli-Juuti, T., Prisle, N.
540 L., Pagels, J., Rarey, J., Zardini, A. A. and Riipinen, I.: Saturation vapor
541 pressures and transition enthalpies of low-volatility organic molecules of
542 atmospheric relevance: from dicarboxylic acids to complex mixtures, Chem.
543 Rev., 115, 4115-4156, https://doi.org/10.1021/cr5005502, 2015.
544 Bosse, D.: Diffusion, viscosity, and thermodynamics in liquid systems, Ph.D. thesis,
545 https://kluedo.ub.uni-kl.de/frontdoor/deliver/index/docId/1691/file/PhD-
546 Bosse-published.pdf, 2005.
547 Cao, W., Knudsen, K., Fredenslund, A. and Rasmussen, P.: Group-contribution
548 viscosity predictions of liquid mixtures using UNIFAC-VLE parameters, Ind.
549 Eng. Chem. Res., 32, 2088–2092, https://doi.org/10.1021/ie00021a034, 1993.
550 Capouet, M. and Müller, J.-F.: A group contribution method for estimating the vapour
551 pressures of α-pinene oxidation products, Atmos. Chem. Phys., 6, 1455-1467,
552 https://doi.org/10.5194/acp-6-1455-2006, 2006.
553 Cappa, C. D. and Jimenez, J. L.: Quantitative estimates of the volatility of ambient
554 organic aerosol, Atmos. Chem. Phys., 10, 5409-5424,
555 https://doi.org/10.5194/acp-10-5409-2010, 2010.
556 Carlton, A. G., de Gouw, J., Jimenez, J. L., Ambrose, J. L., Attwood, A. R., Brown, S.,
557 Baker, K. R., Brock, C., Cohen, R. C. and Edgerton, S.: Synthesis of the
558 southeast atmosphere studies: Investigating fundamental atmospheric chemistry
559 questions, Bull. Amer. Meteor. Soc., 99, 547-567,
560 https://doi.org/10.1175/BAMS-D-16-0048.1, 2018.
561 Cerully, K. M., Bougiatioti, A., Hite Jr, J. R., Guo, H., Xu, L., Ng, N. L., Weber, R. and
562 Nenes, A.: On the link between hygroscopicity, volatility, and oxidation state
563 of ambient and water-soluble aerosols in the southeastern United States, Atmos.
564 Chem. Phys., 15, 8679-8694, https://doi.org/10.5194/acp-15-8679-2015, 2015.
565 Champion, W. M., Rothfuss, N. E., Petters, M. D. and Grieshop, A. P.: Volatility and
566 viscosity are correlated in terpene secondary organic aerosol formed in a flow

https://doi.org/10.5194/acp-2019-1132
Preprint. Discussion started: 6 January 2020

reactor, Environ. Sci. Technol. Lett., 6, 513-519, https://doi.org/10.1021/acs.estlett.9b00412, 2019.

Chenyakin, Y., Ullmann, D. A., Evoy, E., Renbaum-Wolff, L., Kamal, S. and Bertram, A. K.: Diffusion coefficients of organic molecules in sucrose–water solutions and comparison with Stokes–Einstein predictions, Atmos. Chem. Phys., 17, 2423-2435, https://doi.org/10.5194/acp-17-2423-2017, 2017.

Compernolle, S., Ceulemans, K. and Müller, J. F.: EVAPORATION: a new vapour pressure estimation methodfor organic molecules including non-additivity and intramolecular interactions, Atmos. Chem. Phys., 11, 9431-9450, https://doi.org/10.5194/acp-11-9431-2011, 2011.

D'Ambro, E. L., Schobesberger, S., Gaston, C. J., Lopez-Hilfiker, F. D., Lee, B. H., Liu, J., Zelenyuk, A., Bell, D., Cappa, C. D., Helgestad, T., Li, Z., Guenther, A., Wang, J., Wise, M., Caylor, R., Surratt, J. D., Riedel, T., Hyttinen, N., Salo, V. T., Hasan, G., Kurtén, T., Shilling, J. E. and Thornton, J. A.: Chamber-based insights into the factors controlling epoxydiol (IEPOX) secondary organic aerosol (SOA) yield, composition, and volatility, Atmos. Chem. Phys., 19, 11253-11265, https://doi.org/10.5194/acp-19-11253-2019, 2019.

DeRieux, W.-S. W., Lakey, P. S. J., Chu, Y., Chan, C. K. K., Glicker, H., Smith, J. N., Zuend, A. and Shiraiwa, M.: Effects of phase state and phase separation on dimethylamine uptake of ammonium sulfate and ammonium sulfate–sucrose mixed particles, ACS Earth Space Chem., 3, 1268-1278, https://doi.org/10.1021/acsearthspacechem.9b00142, 2019.

DeRieux, W. S. W., Li, Y., Lin, P., Laskin, J., Laskin, A., Bertram, A. K., Nizkorodov, S. A. and Shiraiwa, M.: Predicting the glass transition temperature and viscosity of secondary organic material using molecular composition, Atmos. Chem. Phys., 18, 6331-6351, https://doi.org/10.5194/acp-18-6331-2018, 2018.

Dette, H. P., Qi, M., Schröder, D. C., Godt, A. and Koop, T.: Glass-forming properties of 3-methylbutane-1,2,3-tricarboxylic acid and its mixtures with water and pinonic acid, J. Phys. Chem. A, 118, 7024-7033, https://doi.org/10.1021/jp505910w, 2014.

Dette, H. P. and Koop, T.: Glass formation processes in mixed inorganic/organic aerosol particles, J. Phys. Chem. A, 119, 4552-4561, https://doi.org/10.1021/jp5106967, 2015.

Ditto, J. C., Barnes, E. B., Khare, P., Takeuchi, M., Joo, T., Bui, A. A. T., Lee-Taylor, J., Eris, G., Chen, Y., Aumont, B., Jimenez, J. L., Ng, N. L., Griffin, R. J. and Gentner, D. R.: An omnipresent diversity and variability in the chemical composition of atmospheric functionalized organic aerosol, Commun. Chem., 1, https://doi.org/10.1038/s42004-018-0074-3, 2018.

Ditto, J. C., Joo, T., Khare, P., Sheu, R., Takeuchi, M., Chen, Y., Xu, W., Bui, A. A. T., Sun, Y., Ng, N. L. S. and Gentner, D. R.: Effects of molecular-level compositional variability in organic aerosol on phase state and thermodynamic

https://doi.org/10.5194/acp-2019-1132
Preprint. Discussion started: 6 January 2020

mixing behavior, Environ. Sci. Technol., 53, 13009-13018, https://doi.org/10.1021/acs.est.9b02664, 2019.

Donahue, N., Robinson, A., Stanier, C. and Pandis, S.: Coupled partitioning, dilution, and chemical aging of semivolatile organics, Environ. Sci. Technol., 40, 2635-2643, https://doi.org/10.1021/es052297c, 2006.

Donahue, N., Epstein, S., Pandis, S. and Robinson, A.: A two-dimensional volatility basis set: 1. organic-aerosol mixing thermodynamics, Atmos. Chem. Phys., 11, 3303-3318, https://doi.org/10.5194/acp-11-3303-2011, 2011.

Evoy, E., Maclean, A. M., Rovelli, G., Li, Y., Tsimpidi, A. P., Karydis, V. A., Kamal, S., Lelieveld, J., Shiraiwa, M., Reid, J. P. and Bertram, A. K.: Predictions of diffusion rates of large organic molecules in secondary organic aerosols using the Stokes–Einstein and fractional Stokes–Einstein relations, Atmos. Chem. Phys., 19, 10073-10085, https://doi.org/10.5194/acp-19-10073-2019, 2019.

Faulhaber, A. E., Thomas, B. M., Jimenez, J. L., Jayne, J. T., Worsnop, D. R. and Ziemann, P. J.: Characterization of a thermodenuder-particle beam mass spectrometer system for the study of organic aerosol volatility and composition, Atmos. Meas. Tech., 2, 15-31, https://doi.org/10.5194/amt-2-15-2009, 2009.

Freedman, M. A.: Phase separation in organic aerosol, Chem. Soc. Rev., 46, 7694-7705, https://doi.org/10.1039/c6cs00783j, 2017.

Gervasi, N. R., Topping, D. O. and Zuend, A.: A predictive group-contribution model for the viscosity of aqueous organic aerosol, Atmos. Chem. Phys. Discuss., 2019, 1-32, https://doi.org/10.5194/acp-2019-699, 2019.

Goldstein, A. H. and Galbally, I. E.: Known and unexplored organic constituents in the Earth's atmosphere, Environ. Sci. Technol., 41, 1514-1521, https://doi.org/10.1021/es072476p, 2007.

Gorkowski, K., Preston, T. C. and Zuend, A.: RH-dependent organic aerosol thermodynamics via an efficient reduced-complexity model, Atmos. Chem. Phys., 19, 13383–13407, https://doi.org/10.5194/acp-2019-495, 2019a.

Gorkowski, K., Donahue, N. M., and Sullivan, R. C.: Aerosol optical tweezers constrain the morphology evolution of liquid-liquid phase-separated atmospheric particles, Chem, 6, 1-17, https://doi.org/10.1016/j.chempr.2019.1010.1018, 2019b.

Grayson, J. W., Zhang, Y., Mutzel, A., Renbaum-Wolff, L., Böge, O., Kamal, S., Herrmann, H., Martin, S. T. and Bertram, A. K.: Effect of varying experimental conditions on the viscosity of α-pinene derived secondary organic material, Atmos. Chem. Phys., 16, 6027-6040, https://doi.org/10.5194/acp-16-6027-2016, 2016.

Hallquist, M., Wenger, J., Baltensperger, U., Rudich, Y., Simpson, D., Claeys, M., Dommen, J., Donahue, N., George, C. and Goldstein, A.: The formation, properties and impact of secondary organic aerosol: current and emerging issues, Atmos. Chem. Phys., 9, 5155–5236, https://doi.org/10.5194/acp-9-5155-2009, 2009.

https://doi.org/10.5194/acp-2019-1132
Preprint. Discussion started: 6 January 2020

650 Hu, W. W., Campuzano-Jost, P., Palm, B. B., Day, D. A., Ortega, A. M., Hayes, P. L.,
651 Krechmer, J. E., Chen, Q., Kuwata, M., Liu, Y. J., de Sá, S. S., McKinney, K.,
652 Martin, S. T., Hu, M., Budisulistiorini, S. H., Riva, M., Surratt, J. D., St. Clair,
653 J. M., Isaacman-Van Wertz, G., Yee, L. D., Goldstein, A. H., Carbone, S., Brito,
654 J., Artaxo, P., de Gouw, J. A., Koss, A., Wisthaler, A., Mikoviny, T., Karl, T.,
655 Kaser, L., Jud, W., Hansel, A., Docherty, K. S., Alexander, M. L., Robinson, N.
656 H., Coe, H., Allan, J. D., Canagaratna, M. R., Paulot, F. and Jimenez, J. L.:
657 Characterization of a real-time tracer for isoprene epoxydiols-derived secondary
658 organic aerosol (IEPOX-SOA) from aerosol mass spectrometer measurements,
659 Atmos. Chem. Phys., 15, 11807-11833, https://doi.org/10.5194/acp-15-11807-
660 2015, 2015.
661 Hu, W., Palm, B. B., Day, D. A., Campuzano-Jost, P., Krechmer, J. E., Peng, Z., de Sá,
662 S. S., Martin, S. T., Alexander, M. L., Baumann, K., Hacker, L., Kiendler-
663 Scharr, A., Koss, A. R., de Gouw, J. A., Goldstein, A. H., Seco, R., Sjostedt, S.
664 J., Park, J. H., Guenther, A. B., Kim, S., Canonaco, F., Prévôt, A. S. H., Brune,
665 W. H. and Jimenez, J. L.: Volatility and lifetime against OH heterogeneous
666 reaction of ambient isoprene-epoxydiols-derived secondary organic aerosol
667 (IEPOX-SOA), Atmos. Chem. Phys., 16, 11563-11580,
668 https://doi.org/10.5194/acp-16-11563-2016, 2016.
669 Jain, S., Fischer, B. K. and Petrucci, A. G.: The Influence of absolute mass loading of
670 secondary organic aerosols on their phase state, Atmosphere, 9, 131,
671 https://doi.org/10.3390/atmos9040131, https://doi.org/10.3390/atmos9040131,
672 2018.
673 Jimenez, J. L., Canagaratna, M. R., Donahue, N. M., Prevot, A. S. H., Zhang, Q., Kroll,
674 J. H., DeCarlo, P. F., Allan, J. D., Coe, H., Ng, N. L., Aiken, A. C., Docherty,
675 K. S., Ulbrich, I. M., Grieshop, A. P., Robinson, A. L., Duplissy, J., Smith, J.
676 D., Wilson, K. R., Lanz, V. A., Hueglin, C., Sun, Y. L., Tian, J., Laaksonen, A.,
677 Raatikainen, T., Rautiainen, J., Vaattovaara, P., Ehn, M., Kulmala, M.,
678 Tomlinson, J. M., Collins, D. R., Cubison, M. J., Dunlea, E. J., Huffman, J. A.,
679 Onasch, T. B., Alfarra, M. R., Williams, P. I., Bower, K., Kondo, Y., Schneider,
680 J., Drewnick, F., Borrmann, S., Weimer, S., Demerjian, K., Salcedo, D.,
681 Cottrell, L., Griffin, R., Takami, A., Miyoshi, T., Hatakeyama, S., Shimono, A.,
682 Sun, J. Y., Zhang, Y. M., Dzepina, K., Kimmel, J. R., Sueper, D., Jayne, J. T.,
683 Herndon, S. C., Trimborn, A. M., Williams, L. R., Wood, E. C., Middlebrook,
684 A. M., Kolb, C. E., Baltensperger, U. and Worsnop, D. R.: Evolution of organic
685 aerosols in the atmosphere, Science, 326, 1525-1529,
686 https://doi.org/10.1126/science.1180353, 2009.
687 Jöckel, P., Tost, H., Pozzer, A., Brühl, C., Buchholz, J., Ganzeveld, L., Hoor, P.,
688 Kerkweg, A., Lawrence, M., nbsp, G, Sander, R., Steil, B., Stiller, G., Tanarhte,
689 M., Taraborrelli, D., van Aardenne, J. and Lelieveld, J.: The atmospheric
690 chemistry general circulation model ECHAM5/MESSy1: consistent simulation

https://doi.org/10.5194/acp-2019-1132
Preprint. Discussion started: 6 January 2020

691 of ozone from the surface to the mesosphere, Atmos. Chem. Phys., 6, 5067-
692 5104, https://doi.org/10.5194/acp-6-5067-2006, 2006.
693 Kanakidou, M., Seinfeld, J., Pandis, S., Barnes, I., Dentener, F., Facchini, M.,
694 Dingenen, R. V., Ervens, B., Nenes, A. and Nielsen, C.: Organic aerosol and
695 global climate modelling: a review, Atmos. Chem. Phys., 5, 1053-1123,
696 https://doi.org/10.5194/acp-5-1053-2005, 2005.
697 Kidd, C., Perraud, V., Wingen, L. M. and Finlayson-Pitts, B. J.: Integrating phase and
698 composition of secondary organic aerosol from the ozonolysis of alpha-pinene,
699 Proc. Natl. Acad. Sci. U.S.A., 111, 7552-7557,
700 https://doi.org/10.1073/pnas.1322558111, 2014.
701 Knopf, D. A., Alpert, P. A. and Wang, B.: The role of organic aerosol in atmospheric
702 ice nucleation: a review, ACS Earth Space Chem., 2, 168-202,
703 https://doi.org/10.1021/acsearthspacechem.7b00120, 2018.
704 Koop, T., Bookhold, J., Shiraiwa, M. and Poschl, U.: Glass transition and phase state
705 of organic compounds: dependency on molecular properties and implications
706 for secondary organic aerosols in the atmosphere, Phys. Chem. Chem. Phys.,
707 13, 19238-19255, https://doi.org/10.1039/C1CP22617G, 2011.
708 Kostenidou, E., Karnezi, E., Hite Jr, J. R., Bougiatioti, A., Cerully, K., Xu, L., Ng, N.
709 L., Nenes, A. and Pandis, S. N.: Organic aerosol in the summertime southeastern
710 United States: components and their link to volatility distribution, oxidation
711 state and hygroscopicity, Atmos. Chem. Phys., 18, 5799-5819,
712 https://doi.org/10.5194/acp-18-5799-2018, 2018.
713 Krechmer, J. E., Day, D. A., Ziemann, P. J. and Jimenez, J. L.: Direct measurements of
714 gas/particle partitioning and mass accommodation coefficients in
715 environmental chambers, Environ. Sci. Technol., 51, 11867-11875,
716 https://doi.org/10.1021/acs.est.7b02144, 2017.
717 Krieger, U. K., Marcolli, C. and Reid, J. P.: Exploring the complexity of aerosol particle
718 properties and processes using single particle techniques, Chem. Soc. Rev., 41,
719 6631-6662, https://doi.org/10.1039/C2CS35082C, 2012.
720 Lambe, A. T., Onasch, T. B., Massoli, P., Croasdale, D. R., Wright, J. P., Ahern, A. T.,
721 Williams, L. R., Worsnop, D. R., Brune, W. H. and Davidovits, P.: Laboratory
722 studies of the chemical composition and cloud condensation nuclei (CCN)
723 activity of secondary organic aerosol (SOA) and oxidized primary organic
724 aerosol (OPOA), Atmos. Chem. Phys., 11, 8913-8928,
725 https://doi.org/10.5194/acp-11-8913-2011, 2011.
726 Lee, B.-H., Pierce, J. R., Engelhart, G. J. and Pandis, S. N.: Volatility of secondary
727 organic aerosol from the ozonolysis of monoterpenes, Atmos. Environ., 45,
728 2443-2452, https://doi.org/10.1016/j.atmosenv.2011.02.004, 2011.
729 Lessmeier, J., Dette, H. P., Godt, A. and Koop, T.: Physical state of 2-methylbutane-
730 1,2,3,4-tetraol in pure and internally mixed aerosols, Atmos. Chem. Phys., 18,
731 15841-15857, https://doi.org/10.5194/acp-18-15841-2018, 2018.

https://doi.org/10.5194/acp-2019-1132
Preprint. Discussion started: 6 January 2020

Li, Y., Pöschl, U. and Shiraiwa, M.: Molecular corridors and parameterizations of volatility in the chemical evolution of organic aerosols, Atmos. Chem. Phys., 16, 3327-3344, https://doi.org/10.5194/acp-16-3327-2016, 2016.

Li, Y. and Shiraiwa, M.: Timescales of secondary organic aerosols to reach equilibrium at various temperatures and relative humidities, Atmos. Chem. Phys., 19, 5959-5971, https://doi.org/10.5194/acp-19-5959-2019, 2019.

Lin, Y.-H., Zhang, Z., Docherty, K. S., Zhang, H., Budisulistiorini, S. H., Rubitschun, C. L., Shaw, S. L., Knipping, E. M., Edgerton, E. S., Kleindienst, T. E., Gold, A. and Surratt, J. D.: Isoprene epoxydiols as precursors to secondary organic aerosol formation: acid-catalyzed reactive uptake studies with authentic compounds, Environ. Sci. Technol., 46, 250-258, https://doi.org/10.1021/es202554c, 2012.

Lin, Y.-H., Zhang, H., Pye, H. O. T., Zhang, Z., Marth, W. J., Park, S., Arashiro, M., Cui, T., Budisulistiorini, S. H., Sexton, K. G., Vizuete, W., Xie, Y., Luecken, D. J., Piletic, I. R., Edney, E. O., Bartolotti, L. J., Gold, A. and Surratt, J. D.: Epoxide as a precursor to secondary organic aerosol formation from isoprene photooxidation in the presence of nitrogen oxides, Proc. Natl. Acad. Sci. U.S.A., 110, 6718-6723, https://doi.org/10.1073/pnas.1221150110, 2013.

Liu, P., Li, Y. J., Wang, Y., Gilles, M. K., Zaveri, R. A., Bertram, A. K. and Martin, S. T.: Lability of secondary organic particulate matter, Proc. Natl. Acad. Sci. U.S.A., 113, 12643-12648, https://doi.org/10.1021/10.1021/acscentsci.7b00452, 2016.

Liu, X., Day, D. A., Krechmer, J. E., Brown, W., Peng, Z., Ziemann, P. J. and Jimenez, J. L.: Direct measurements of semi-volatile organic compound dynamics show near-unity mass accommodation coefficients for diverse aerosols, Commun. Chem., 2, https://doi.org/10.1038/s42004-019-0200-x, 2019.

Liu, Y., Wu, Z., Wang, Y., Xiao, Y., Gu, F., Zheng, J., Tan, T., Shang, D., Wu, Y., Zeng, L., Hu, M., Bateman, A. P. and Martin, S. T.: Submicrometer particles are in the liquid state during heavy haze episodes in the urban atmosphere of Beijing, China, Environ. Sci. Technol. Lett., 4, 427-432, https://doi.org/10.1021/acs.estlett.7b00352, 2017.

Lopez-Hilfiker, F. D., Mohr, C., Ehn, M., Rubach, F., Kleist, E., Wildt, J., Mentel, T. F., Lutz, A., Hallquist, M., Worsnop, D. and Thornton, J. A.: A novel method for online analysis of gas and particle composition: description and evaluation of a Filter Inlet for Gases and AEROsols (FIGAERO), Atmos. Meas. Tech., 7, 983-1001, https://doi.org/10.5194/amt-7-983-2014, 2014.

Lopez-Hilfiker, F. D., Mohr, C., D'Ambro, E. L., Lutz, A., Riedel, T. P., Gaston, C. J., Iyer, S., Zhang, Z., Gold, A., Surratt, J. D., Lee, B. H., Kurten, T., Hu, W. W., Jimenez, J., Hallquist, M. and Thornton, J. A.: Molecular composition and volatility of organic aerosol in the southeastern U.S.: implications for IEPOX derived SOA, Environ. Sci. Technol., 50, 2200-2209, https://doi.org/10.1021/acs.est.5b04769, 2016.

https://doi.org/10.5194/acp-2019-1132
Preprint. Discussion started: 6 January 2020

774 Loza, C. L., Coggon, M. M., Nguyen, T. B., Zuend, A., Flagan, R. C. and Seinfeld, J.
775 H.: On the mixing and evaporation of secondary organic aerosol components,
776 Environ. Sci. Technol., 47, 6173-6180, https://doi.org/ 10.1021/es400979k,
777 2013.
778 Marshall, F. H., Berkemeier, T., Shiraiwa, M., Nandy, L., Ohm, P. B., Dutcher, C. S.
779 and Reid, J. P.: Influence of particle viscosity on mass transfer and
780 heterogeneous ozonolysis kinetics in aqueous-sucrose-maleic acid aerosol,
781 Phys. Chem. Chem. Phys., 20, 15560-15573,
782 https://doi.org/10.1039/c8cp01666f, 2018.
783 Mikhailov, E., Vlasenko, S., Martin, S. T., Koop, T. and Pöschl, U.: Amorphous and
784 crystalline aerosol particles interacting with water vapor: conceptual framework
785 and experimental evidence for restructuring, phase transitions and kinetic
786 limitations, Atmos. Chem. Phys., 9, 9491-9522, https://doi.org/10.5194/acp-9-
787 9491-2009, 2009.
788 Nizkorodov, S. A., Laskin, J. and Laskin, A.: Molecular chemistry of organic aerosols
789 through the application of high resolution mass spectrometry, Phys. Chem.
790 Chem. Phys., 13, 3612-3629, https://doi.org/10.1039/c0cp02032j, 2011.
791 O'Brien, R. E., Neu, A., Epstein, S. A., MacMillan, A. C., Wang, B., Kelly, S. T.,
792 Nizkorodov, S. A., Laskin, A., Moffet, R. C. and Gilles, M. K.: Physical
793 properties of ambient and laboratory-generated secondary organic aerosol,
794 Geophys. Res. Lett., 41, 4347-4353, https://doi.org/10.1002/2014GL060219,
795 2014.
796 O'Meara, S., Booth, A. M., Barley, M. H., Topping, D. and McFiggans, G.: An
797 assessment of vapour pressure estimation methods, Phys.Chem.Chem.Phys.,
798 16, 19453-19469, https://doi.org/10.1039/c4cp00857j, 2014.
799 Paciga, A., Karnezi, E., Kostenidou, E., Hildebrandt, L., Psichoudaki, M., Engelhart,
800 G. J., Lee, B. H., Crippa, M., Prévôt, A. S. H., Baltensperger, U. and Pandis, S.
801 N.: Volatility of organic aerosol and its components in the megacity of Paris,
802 Atmos. Chem. Phys., 16, 2013-2023, https://doi.org/10.5194/acp-16-2013-
803 2016, 2016.
804 Pajunoja, A., Hu, W., Leong, Y. J., Taylor, N. F., Miettinen, P., Palm, B. B., Mikkonen,
805 S., Collins, D. R., Jimenez, J. L. and Virtanen, A.: Phase state of ambient aerosol
806 linked with water uptake and chemical aging in the southeastern US, Atmos.
807 Chem. Phys., 16, 11163-11176, https://doi.org/10.5194/acp-16-11163-2016,
808 2016.
809 Pajunoja, A., Malila, J., Hao, L., Joutsensaari, J., Lehtinen, K. E. and Virtanen, A.:
810 Estimating the viscosity range of SOA particles based on their coalescence time,
811 Aerosol Sci. Technol., 48, https://doi.org/10.1080/02786826.2013.870325,
812 2014.
813 Pankow, J. F.: An absorption model of gas-particle partitioning of organic-compounds
814 in the atmosphere, Atmos. Environ., 28, 185-188, https://doi.org/10.1016/1352-
815 2310(94)90093-0, 1994.

https://doi.org/10.5194/acp-2019-1132
Preprint. Discussion started: 6 January 2020

Pankow, J. F. and Asher, W. E.: SIMPOL.1: a simple group contribution method for predicting vapor pressures and enthalpies of vaporization of multifunctional organic compounds, Atmos. Chem. Phys., 8, 2773-2796, https://doi.org/10.5194/acp-8-2773-2008, 2008.

Perraud, V., Bruns, E. A., Ezell, M. J., Johnson, S. N., Yu, Y., Alexander, M. L., Zelenyuk, A., Imre, D., Chang, W. L., Dabdub, D., Pankow, J. F. and Finlayson-Pitts, B. J.: Nonequilibrium atmospheric secondary organic aerosol formation and growth, Proc. Natl. Acad. Sci. U.S.A., 109, 2836-2841, https://doi.org/10.1073/pnas.1119909109, 2012.

Petters, M. D. and Kreidenweis, S. M.: A single parameter representation of hygroscopic growth and cloud condensation nucleus activity, Atmos. Chem. Phys., 7, 1961-1971, https://doi.org/10.5194/acp-7-1961-2007, 2007.

Petters, S. S., Kreidenweis, S. M., Grieshop, A. P., Ziemann, P. J. and Petters, M. D.: Temperature- and humidity-dependent phase states of secondary organic aerosols, Geophys. Res. Lett., 46, https://doi.org/10.1029/2018GL080563, 2019.

Pöschl, U. and Shiraiwa, M.: Multiphase chemistry at the atmosphere-biosphere interface influencing climate and public health in the anthropocene, Chem. Rev., 115, 4440-4475, https://doi.org/10.1021/cr500487s, 2015.

Price, H. C., Mattsson, J. and Murray, B. J.: Sucrose diffusion in aqueous solution, Phys. Chem. Chem. Phys., 18, 19207-19216, https://doi.org/10.1039/c6cp03238a, 2016.

Pringle, K. J., Tost, H., Pozzer, A., Pöschl, U. and Lelieveld, J.: Global distribution of the effective aerosol hygroscopicity parameter for CCN activation, Atmos. Chem. Phys., 10, 5241-5255, https://doi.org/10.5194/acp-10-5241-2010, 2010.

Pye, H. O. T., Murphy, B. N., Xu, L., Ng, N. L., Carlton, A. G., Guo, H., Weber, R., Vasilakos, P., Appel, K. W., Budisulistiorini, S. H., Surratt, J. D., Nenes, A., Hu, W., Jimenez, J. L., Isaacman-VanWertz, G., Misztal, P. K. and Goldstein, A. H.: On the implications of aerosol liquid water and phase separation for organic aerosol mass, Atmos. Chem. Phys., 17, 343-369, https://doi.org/10.5194/acp-17-343-2017, 2017.

Reid, J. P., Bertram, A. K., Topping, D. O., Laskin, A., Martin, S. T., Petters, M. D., Pope, F. D. and Rovelli, G.: The viscosity of atmospherically relevant organic particles, Nat. Commun., 9, 956, https://doi.org/10.1038/s41467-018-03027-z, 2018.

Renbaum-Wolff, L., Grayson, J. W., Bateman, A. P., Kuwata, M., Sellier, M., Murray, B. J., Shilling, J. E., Martin, S. T. and Bertram, A. K.: Viscosity of α-pinene secondary organic material and implications for particle growth and reactivity, Proc. Natl. Acad. Sci. U.S.A., 110, 8014-8019, https://doi.org/10.1073/pnas.1219548110, 2013.

Riva, M., Chen, Y., Zhang, Y., Lei, Z., Olson, N. E., Boyer, H. C., Narayan, S., Yee, L. D., Green, H. S., Cui, T., Zhang, Z., Baumann, K., Fort, M., Edgerton, E.,

https://doi.org/10.5194/acp-2019-1132
Preprint. Discussion started: 6 January 2020

Budisulistiorini, S. H., Rose, C. A., Ribeiro, I. O., e Oliveira, R. L., dos Santos, E. O., Machado, C. M. D., Szopa, S., Zhao, Y., Alves, E. G., de Sá, S. S., Hu, W., Knipping, E. M., Shaw, S. L., Duvoisin Junior, S., de Souza, R. A. F., Palm, B. B., Jimenez, J.-L., Glasius, M., Goldstein, A. H., Pye, H. O. T., Gold, A., Turpin, B. J., Vizuete, W., Martin, S. T., Thornton, J. A., Dutcher, C. S., Ault, A. P. and Surratt, J. D.: Increasing isoprene epoxydiol-to-inorganic sulfate aerosol ratio results in extensive conversion of inorganic sulfate to organosulfur forms: implications for aerosol physicochemical properties, Environ. Sci. Technol., 53, 8682-8694, https://doi.org/10.1021/acs.est.9b01019, 2019.

Rothfuss, N. E. and Petters, M. D.: I nfluence of functional groups on the viscosity of organic aerosol, Environ. Sci. Technol., 51, 271-279, https://doi.org/10.1021/acs.est.6b04478, 2017.

Rovelli, G., Song, Y.-C., Maclean, A. M., Topping, D. O., Bertram, A. K. and Reid, J. P.: Comparison of approaches for measuring and predicting the viscosity of ternary component aerosol particles, Anal. Chem., 91, 5074-5082, https://doi.org/10.1021/acs.analchem.8b05353, 2019.

Saha, P. K., Khlystov, A., Yahya, K., Zhang, Y., Xu, L., Ng, N. L. and Grieshop, A. P.: Quantifying the volatility of organic aerosol in the southeastern US, Atmos. Chem. Phys., 17, 501-520, https://doi.org/10.5194/acp-17-501-2017, 2017.

Saha, P. K., Khlystov, A. and Grieshop, A. P.: Downwind evolution of the volatility and mixing state of near-road aerosols near a US interstate highway, Atmos. Chem. Phys., 18, 2139-2154, https://doi.org/10.5194/acp-18-2139-2018, 2018.

Saukko, E., Lambe, A. T., Massoli, P., Koop, T., Wright, J. P., Croasdale, D. R., Pedernera, D. A., Onasch, T. B., Laaksonen, A., Davidovits, P., Worsnop, D. R. and Virtanen, A.: Humidity-dependent phase state of SOA particles from biogenic and anthropogenic precursors, Atmos. Chem. Phys., 12, 7517-7529, https://doi.org/10.5194/acp-12-7517-2012, 2012.

Schmedding, R., Rasool, Q. Z., Zhang, Y., Pye, H. O. T., Zhang, H., Chen, Y., Surratt, J. D., Lee, B. H., Mohr, C., Lopez-Hilfiker, F. D., Thornton, J. A., Goldstein, A. H. and Vizuete, W.: Predicting secondary organic aerosol phase state and viscosity and its effect on multiphase chemistry in a regional scale air quality model, Atmos. Chem. Phys. Discuss., 2019, 1-59, https://doi.org/10.5194/acp-2019-900, 2019.

Schum, S. K., Zhang, B., Džepina, K., Fialho, P., Mazzoleni, C. and Mazzoleni, L. R.: Molecular and physical characteristics of aerosol at a remote free troposphere site: implications for atmospheric aging, Atmos. Chem. Phys., 18, 14017-14036, https://doi.org/10.5194/acp-18-14017-2018, 2018.

Seinfeld, J. H. and Pandis, S. N.: Atmospheric chemistry and physics - From air pollution to climate change, John Wiley & Sons, Inc., New York, 2006.

Shiraiwa, M., Ammann, M., Koop, T. and Poschl, U.: Gas uptake and chemical aging of semisolid organic aerosol particles, Proc. Natl. Acad. Sci. U.S.A., 108, 11003-11008, https://doi.org/10.1073/pnas.1103045108, 2011.

https://doi.org/10.5194/acp-2019-1132
Preprint. Discussion started: 6 January 2020

900 Shiraiwa, M. and Seinfeld, J. H.: Equilibration timescale of atmospheric secondary
901 organic aerosol partitioning, Geophys. Res. Lett., 39,
902 https://doi.org/10.1029/2012GL054008, 2012.
903 Shiraiwa, M., Berkemeier, T., Schilling-Fahnestock, K. A., Seinfeld, J. H. and Pöschl,
904 U.: Molecular corridors and kinetic regimes in the multiphase chemical
905 evolution of secondary organic aerosol, Atmos. Chem. Phys., 14, 8323-8341,
906 https://doi.org/10.5194/acp-14-8323-2014, 2014.
907 Shiraiwa, M., Li, Y., Tsimpidi, A. P., Karydis, V. A., Berkemeier, T., Pandis, S. N.,
908 Lelieveld, J., Koop, T. and Pöschl, U.: Global distribution of particle phase state
909 in atmospheric secondary organic aerosols, Nat. Commun., 8, 15002,
910 https://doi.org/10.1038/ncomms15002, 2017.
911 Shrivastava, M., Cappa, C. D., Fan, J., Goldstein, A. H., Guenther, A. B., Jimenez, J.
912 L., Kuang, C., Laskin, A., Martin, S. T., Ng, N. L., Petaja, T., Pierce, J. R.,
913 Rasch, P. J., Roldin, P., Seinfeld, J. H., Shilling, J., Smith, J. N., Thornton, J.
914 A., Volkamer, R., Wang, J., Worsnop, D. R., Zaveri, R. A., Zelenyuk, A. and
915 Zhang, Q.: Recent advances in understanding secondary organic aerosol:
916 Implications for global climate forcing, Rev. Geophys., 55, 509-559,
917 https://doi.org/10.1002/2016RG000540, 2017.
918 Slade, J. H., Ault, A. P., Bui, A. T., Ditto, J. C., Lei, Z., Bondy, A. L., Olson, N. E.,
919 Cook, R. D., Desrochers, S. J., Harvey, R. M., Erickson, M. H., Wallace, H. W.,
920 Alvarez, S. L., Flynn, J. H., Boor, B. E., Petrucci, G. A., Gentner, D. R., Griffin,
921 R. J. and Shepson, P. B.: Bouncier particles at night: biogenic secondary organic
922 aerosol chemistry and sulfate drive diel variations in the aerosol phase in a
923 mixed forest, Environ. Sci. Technol., 53, 4977-4987,
924 https://doi.org/10.1021/acs.est.8b07319, 2019.
925 Song, M., Liu, P. F., Hanna, S. J., Li, Y. J., Martin, S. T. and Bertram, A. K.: Relative
926 humidity-dependent viscosities of isoprene-derived secondary organic material
927 and atmospheric implications for isoprene-dominant forests, Atmos. Chem.
928 Phys., 15, 5145-5159, https://doi.org/10.5194/acp-15-5145-2015, 2015.
929 Song, M., Liu, P. F., Hanna, S. J., Zaveri, R. A., Potter, K., You, Y., Martin, S. T. and
930 Bertram, A. K.: Relative humidity-dependent viscosity of secondary organic
931 material from toluene photo-oxidation and possible implications for organic
932 particulate matter over megacities, Atmos. Chem. Phys., 16, 8817-8830,
933 https://doi.org/10.5194/acp-16-8817-2016, 2016a.
934 Song, M., Maclean, A. M., Huang, Y., Smith, N. R., Blair, S. L., Laskin, J., Laskin, A.,
935 DeRieux, W. S. W., Li, Y., Shiraiwa, M., Nizkorodov, S. A. and Bertram, A.
936 K.: Liquid-liquid phase separation and viscosity within secondary organic
937 aerosol generated from diesel fuel vapors, Atmos. Chem. Phys., 19, 12515–
938 12529, https://doi.org/10.5194/acp-2019-367, 2019.
939 Song, Y. C., Haddrell, A. E., Bzdek, B. R., Reid, J. P., Bannan, T., Topping, D. O.,
940 Percival, C. and Cai, C.: Measurements and predictions of binary component

https://doi.org/10.5194/acp-2019-1132
Preprint. Discussion started: 6 January 2020

aerosol particle viscosity, J. Phys. Chem. A, 120, 8123-8137, https://doi.org/10.1021/acs.jpca.6b07835, 2016b.

Stark, H., Yatavelli, R. L. N., Thompson, S. L., Kimmel, J. R., Cubison, M. J., Chhabra, P. S., Canagaratna, M. R., Jayne, J. T., Worsnop, D. R. and Jimenez, J. L.: Methods to extract molecular and bulk chemical information from series of complex mass spectra with limited mass resolution, Int. J. Mass Spectrom., 389, 26-38, https://doi.org/10.1016/j.ijms.2015.08.011, 2015.

Stark, H., Yatavelli, R. L., Thompson, S. L., Kang, H., Krechmer, J. E., Kimmel, J. R., Palm, B. B., Hu, W., Hayes, P. L. and Day, D. A.: Impact of thermal decomposition on thermal desorption instruments: advantage of thermogram analysis for quantifying volatility distributions of organic species, Environ. Sci. Technol., 51, 8491-8500, https://doi.org/10.1021/acs.est.7b00160, 2017.

Surratt, J. D., Chan, A. W. H., Eddingsaas, N. C., Chan, M., Loza, C. L., Kwan, A. J., Hersey, S. P., Flagan, R. C., Wennberg, P. O. and Seinfeld, J. H.: Reactive intermediates revealed in secondary organic aerosol formation from isoprene, Proc. Natl. Acad. Sci. U.S.A., 107, 6640-6645, https://doi.org/10.1073/pnas.0911114107, 2010.

Thomas, L. H., Meatyard, R., Smith, H. and Davies, G. H.: Viscosity behavior of associated liquids at lower temperatures and vapor pressures, J. Chem. Eng. Data, 24, 161-164, https://doi.org/10.1021/je60082a011, 1979.

Thompson, S. L., Yatavelli, R. L. N., Stark, H., Kimmel, J. R., Krechmer, J. E., Day, D. A., Hu, W., Isaacman-VanWertz, G., Yee, L., Goldstein, A. H., Khan, M. A. H., Holzinger, R., Kreisberg, N., Lopez-Hilfiker, F. D., Mohr, C., Thornton, J. A., Jayne, J. T., Canagaratna, M., Worsnop, D. R. and Jimenez, J. L.: Field intercomparison of the gas/particle partitioning of oxygenated organics during the Southern Oxidant and Aerosol Study (SOAS) in 2013, Aerosol Sci. Tech., 51, 30-56, https://doi.org/10.1080/02786826.2016.1254719, 2017.

Tsimpidi, A. P., Karydis, V. A., Pozzer, A., Pandis, S. N. and Lelieveld, J.: ORACLE (v1.0): module to simulate the organic aerosol composition and evolution in the atmosphere, Geosci. Model Dev., 7, 3153-3172, https://doi.org/10.5194/gmd-7-3153-2014, 2014.

US EPA: Estimation Programs Interface Suite™ for Microsoft Windows v4.1, United States Environmental Protection Agency, Washington, DC, USA, 2015.

Vander Wall, A. C., Lakey, P. S. J., Rossich Molina, E., Perraud, V., Wingen, L. M., Xu, J., Soulsby, D., Gerber, R. B., Shiraiwa, M. and Finlayson-Pitts, B. J.: Understanding interactions of organic nitrates with the surface and bulk of organic films: implications for particle growth in the atmosphere, Environ. Sci. Processes Impacts, 20, 1593-1610, https://doi.org/10.1039/C8EM00348C, 2018.

Virtanen, A., Joutsensaari, J., Koop, T., Kannosto, J., YliPirilä, P., Leskinen, J., Mäkelä, J. M., Holopainen, J. K., Pöschl, U., Kulmala, M., Worsnop, D. R. and

https://doi.org/10.5194/acp-2019-1132
Preprint. Discussion started: 6 January 2020

Laaksonen, A.: An amorphous solid state of biogenic secondary organic aerosol particles, Nature, 467, 824-827, https://doi.org/10.1038/nature09455, 2010.

Xu, L., Suresh, S., Guo, H., Weber, R. J. and Ng, N. L.: Aerosol characterization over the southeastern United States using high-resolution aerosol mass spectrometry: spatial and seasonal variation of aerosol composition and sources with a focus on organic nitrates, Atmos. Chem. Phys., 15, 7307-7336, https://doi.org/10.5194/acp-15-7307-2015, 2015.

Xu, W., Xie, C., Karnezi, E., Zhang, Q., Wang, J., Pandis, S. N., Ge, X., Zhang, J., An, J., Wang, Q., Zhao, J., Du, W., Qiu, Y., Zhou, W., He, Y., Li, Y., Li, J., Fu, P., Wang, Z., Worsnop, D. R. and Sun, Y.: Summertime aerosol volatility measurements in Beijing, China, Atmos. Chem. Phys., 19, https://doi.org/10205-10216, 10.5194/acp-19-10205-2019, 2019.

Yatavelli, R. L. N., Mohr, C., Stark, H., Day, D. A., Thompson, S. L., Lopez-Hilfiker, F. D., Campuzano-Jost, P., Palm, B. B., Vogel, A. L., Hoffmann, T., Heikkinen, L., Äijälä, M., Ng, N. L., Kimmel, J. R., Canagaratna, M. R., Ehn, M., Junninen, H., Cubison, M. J., Petäjä, T., Kulmala, M., Jayne, J. T., Worsnop, D. R. and Jimenez, J. L.: Estimating the contribution of organic acids to northern hemispheric continental organic aerosol, Geophys. Res. Lett., 42, 6084-6090, https://doi.org/10.1002/2015gl064650, 2015.

Ye, Q., Upshur, M. A., Robinson, E. S., Geiger, F. M., Sullivan, R. C., Thomson, R. J. and Donahue, N. M.: Following particle-particle mixing in atmospheric secondary organic aerosols by using isotopically labeled terpenes, Chem, 4, 318-333, https://doi.org/10.1016/j.chempr.2017.12.008, 2018.

Yli-Juuti, T., Pajunoja, A., Tikkanen, O.-P., Buchholz, A., Faiola, C., Väisänen, O., Hao, L., Kari, E., Peräkylä, O., Garmash, O., Shiraiwa, M., Ehn, M., Lehtinen, K. and Virtanen, A.: Factors controlling the evaporation of secondary organic aerosol from α-pinene ozonolysis, Geophys. Res. Lett., 44, 2562-2570, https://doi.org/10.1002/2016GL072364, 2017.

Zaveri, R. A., Shilling, J. E., Zelenyuk, A., Liu, J., Bell, D. M., D'Ambro, E. L., Gaston, C. J., Thornton, J. A., Laskin, A., Lin, P., Wilson, J., Easter, R. C., Wang, J., Bertram, A. K., Martin, S. T., Seinfeld, J. H. and Worsnop, D. R.: Growth kinetics and size distribution dynamics of viscous secondary organic aerosol, Environ. Sci. Technol., 52, 1191-1199, https://doi.org/10.1021/acs.est.7b04623, 2018.

Zhang, Y., Sanchez, M. S., Douet, C., Wang, Y., Bateman, A. P., Gong, Z., Kuwata, M., Renbaum-Wolff, L., Sato, B. B., Liu, P. F., Bertram, A. K., Geiger, F. M. and Martin, S. T.: Changing shapes and implied viscosities of suspended submicron particles, Atmos. Chem. Phys., 15, 7819-7829, https://doi.org/10.5194/acp-15-7819-2015, 2015.

Zhang, Y., Katira, S., Lee, A., Lambe, A. T., Onasch, T. B., Xu, W., Brooks, W. A., Canagaratna, M. R., Freedman, A. and Jayne, J. T.: Kinetically controlled glass transition measurement of organic aerosol thin films using broadband dielectric

https://doi.org/10.5194/acp-2019-1132
Preprint. Discussion started: 6 January 2020

spectroscopy, Atmos. Meas. Tech., 11, 3479–3490, https://doi.org/10.5194/amt-11-3479-2018, 2018.

Zhang, Y., Nichman, L., Spencer, P., Jung, J. I., Lee, A., Heffernan, B. K., Gold, A., Zhang, Z., Chen, Y., Canagaratna, M. R., Jayne, J. T., Worsnop, D. R., Onasch, T. B., Surratt, J. D., Chandler, D., Davidovits, P. and Kolb, C. E.: The cooling rate and volatility dependent glass forming properties of organic aerosols measured by Broadband Dielectric Spectroscopy, Environ. Sci. & Technol., 53, 12366-12378, https://doi.org/10.1021/acs.est.9b03317, 2019.

Zhou, S., Hwang, B. C. H., Lakey, P. S. J., Zuend, A., Abbatt, J. P. D. and Shiraiwa, M.: Multiphase reactivity of polycyclic aromatic hydrocarbons is driven by phase separation and diffusion limitations, Proc. Natl. Acad. Sci. U.S.A., 116, 11658-11663, https://doi.org/10.1073/pnas.1902517116, 2019.

Zobrist, B., Marcolli, C., Pedernera, D. and Koop, T.: Do atmospheric aerosols form glasses?, Atmos. Chem. Phys., 8, 5221-5244, https://doi.org/10.5194/acp-8-5221-2008, 2008.

Zuend, A. and Seinfeld, J. H.: Modeling the gas-particle partitioning of secondary organic aerosol: the importance of liquid-liquid phase separation, Atmos. Chem. Phys., 12, 3857-3882, https://doi.org/10.5194/acp-12-3857-2012, 2012.

https://doi.org/10.5194/acp-2019-1132
Preprint. Discussion started: 6 January 2020

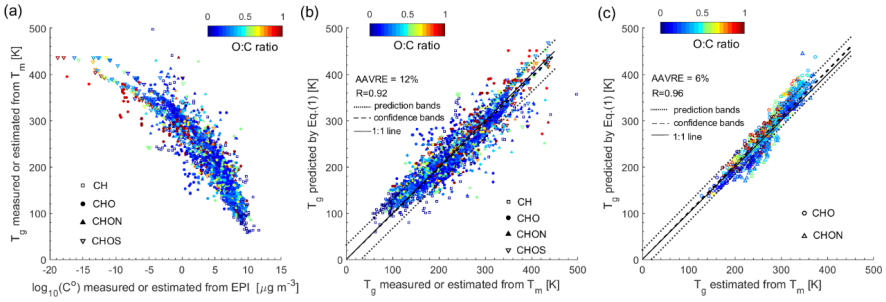

Figure 1. (a) T_g of organic compounds as measured and estimated by the melting temperature (T_m) with the Boyer-Kauzmann rule plotted against pure compound saturation mass concentration (C^0) as measured and estimated from the EPI suite (see supplement for details of the dataset). (b) Predicted T_g for compounds shown in (a) using a parameterization (Eq. 1) developed in this study compared to measured and estimated T_g from T_m with the Boyer-Kauzmann rule. (c) Predicted T_g for SOA components (Shiraiwa et al., 2014) using Eq. (1) plotted against estimated T_g from T_m with the Boyer-Kauzmann rule. The markers are color-coded by the atomic O:C ratio. Organic compounds include CH compounds (squares), CHO compounds (circles), CHON compounds (triangles), and CHOS compounds (inverted triangles). The correlation coefficient (R) and the average absolute value of the relative error (AAVRE) are shown. The solid line shows the 1:1 line and the dashed and dotted lines show 68% confidence and prediction bands, respectively.

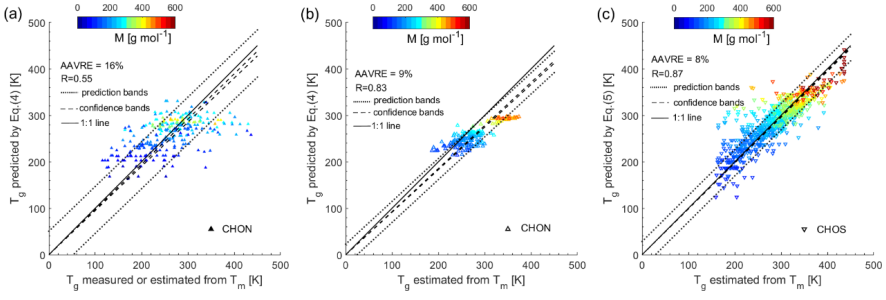

Figure 2. (a) Predicted T_g for CHON compounds using a parameterization (Eq. 4) developed in this study compared to measured or estimated T_g by the Boyer-Kauzmann rule using measured T_m. (b) Predicted T_g for CHON compounds using Eq. (4) compared to estimated T_g by the Boyer-Kauzmann rule with T_m estimated by the EPI suite. (c) Predicted T_g for CHOS compounds using Eq. (5) compared to estimated T_g by the Boyer-Kauzmann rule with T_m estimated by the EPI suite. The markers are color-coded by the molar mass. The solid line shows the 1:1 line and the dashed and dotted lines show 68% confidence and prediction bands, respectively. The correlation coefficient (R) and the average absolute value of the relative error (AAVRE) are included in each figure legend.

https://doi.org/10.5194/acp-2019-1132
Preprint. Discussion started: 6 January 2020

Atmospheric Chemistry and Physics Discussions

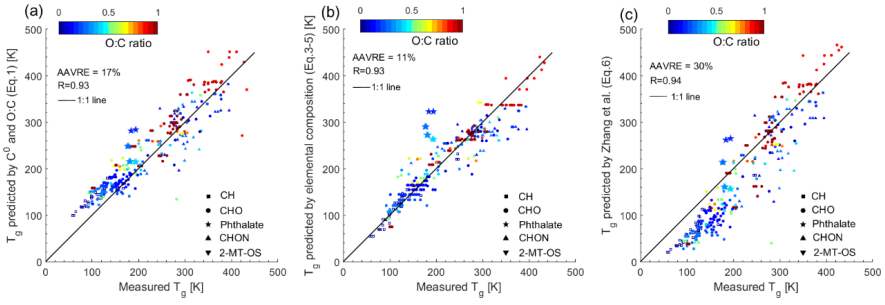

Figure 3. Comparison between measured T_g and T_g predicted by (a) C^0 and O:C (Eq. 1), (b) elemental composition (Eqs. 3-5), and (c) the parameterization (Eq. 6) in Zhang et al. (2019). The markers are color-coded by the atomic O:C ratio. The solid line shows the 1:1 line. The compounds include CH compounds (squares), CHO compounds (circles), phthalates (stars), CHON compounds (triangles), and 2-methyltetrol sulfates (2-MT-OS, inverted triangle). The correlation coefficient (R) and the average absolute value of the relative error (AAVRE) are included in each figure legend.

https://doi.org/10.5194/acp-2019-1132
Preprint. Discussion started: 6 January 2020

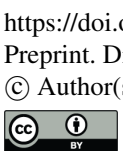

Atmospheric Chemistry and Physics Discussions

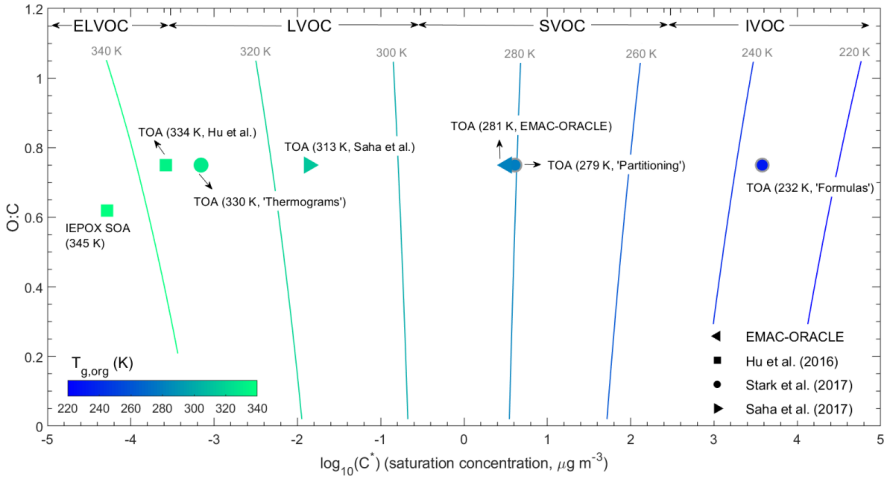

Figure 4. Predicted glass transition temperatures of organic aerosols under dry conditions ($T_{g,org}$) during the SOAS campaign, which are placed into the two-dimensional VBS framework. The isopleths correspond to the $T_{g,org}$ calculated using Eq (1) with the effective saturation mass concentration (C^*) and the O:C ratio defined in the 2D-VBS. The markers represent the $T_{g,org}$ of total OA (TOA) and IEPOX SOA calculated from the volatility distributions simulated by a global chemical transport model EMAC-ORACLE (Shiraiwa et al., 2017) or measured during the SOAS campaign (Hu et al., 2016; Saha et al., 2017; Stark et al., 2017). Three methods ('Formulas', 'Partitioning', and 'Thermograms') are applied in Stark et al. (2017) to derive the C^* distributions, while the "Thermograms" method provides the most credible volatility distributions compared to 'Formulas' and 'Partitioning' (edge lines are in gray).

https://doi.org/10.5194/acp-2019-1132
Preprint. Discussion started: 6 January 2020

Atmospheric Chemistry and Physics Discussions

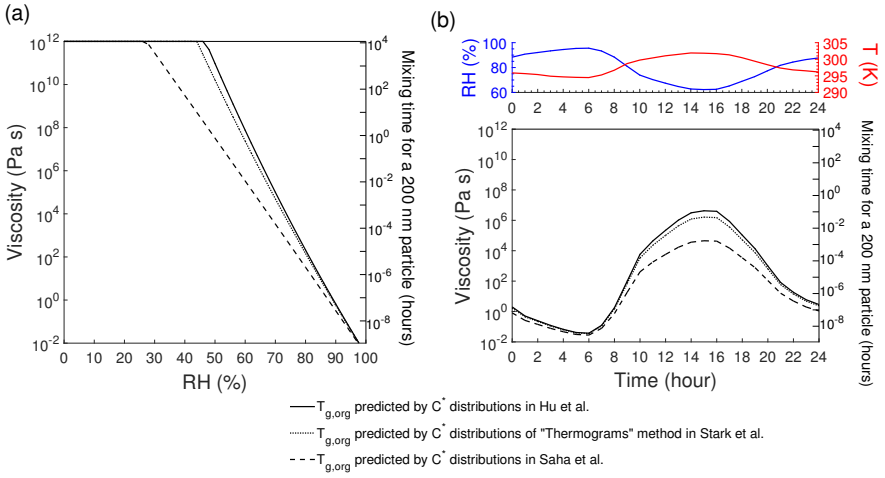

Figure 5. (a) Predicted viscosity of total OA measured during the SOAS campaign as a function of RH. (b) Diurnal variations of viscosity of total OA predicted employing the measured RH and T (Hu et al., 2016) during the SOAS campaign. $T_{g,org}$ are calculated using the volatility distributions measured in Hu et al., (2016), Saha et al. (2017), and the "Thermograms" method in Stark et al. (2017). Characteristic mixing timescales of organic molecules with the radius of 10^{-10} m within 200 nm particles are also shown in the right axis.

https://doi.org/10.5194/acp-2019-1132
Preprint. Discussion started: 6 January 2020

Atmospheric Chemistry and Physics Discussions

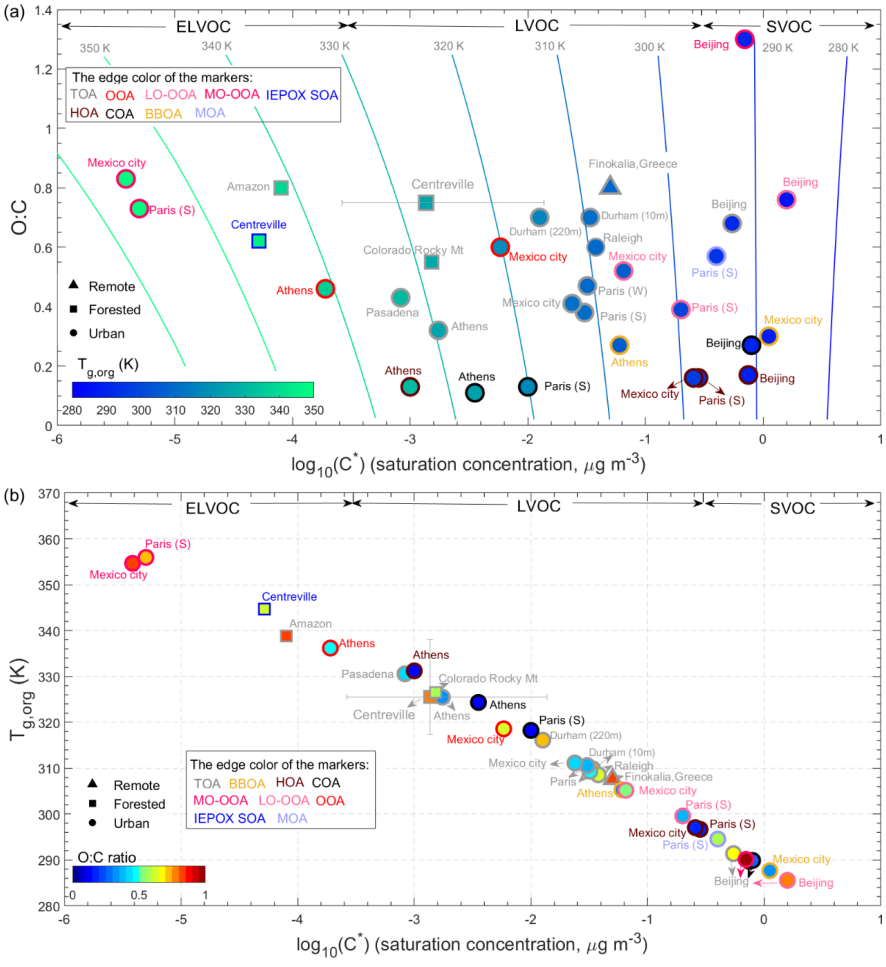

Figure 6. Predicted glass transition temperatures of organic aerosols under dry conditions ($T_{g,org}$) at 11 sites. The isopleths in (a) correspond to the T_g varied with the effective saturation mass concentration (C^*) and the O:C ratio in the two-dimensional VBS (2D-VBS) framework. The markers represent the $T_{g,org}$ of total OA (TOA) and its components calculated from measured volatility distributions (Table S2) and color-coded with $T_{g,org}$ in (a) and the O:C ratio in (b). The edge color of the markers indicates the OA components identified via positive matrix factorization (PMF) of aerosol mass spectrometer data.

https://doi.org/10.5194/acp-2019-1132
Preprint. Discussion started: 6 January 2020

Atmospheric Chemistry and Physics Discussions

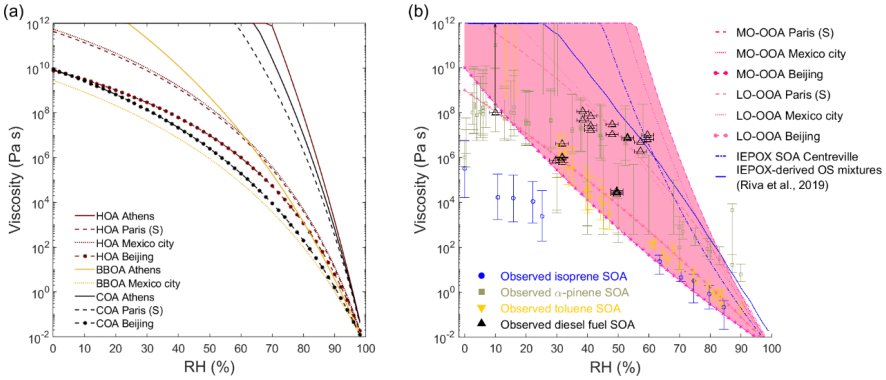

Figure 7. Predicted viscosity of (a) HOA, COA and BBOA and (b) LO-OOA, MO-OOA, IEPOX SOA and Isoprene OA in different locations at 298 K as a function of RH. Experimentally measured viscosity of laboratory-generated SOA formed from isoprene (Song et al., 2015), α-pinene (Abramson et al., 2013; Renbaum-Wolff et al., 2013; Kidd et al., 2014; Pajunoja et al., 2014; Bateman et al., 2015; Zhang et al., 2015; Grayson et al., 2016; Petters et al., 2019), toluene (Song et al., 2016), and diesel fuel (Song et al., 2019) are also shown. Predicted viscosity of IEPOX-derived OS mixtures (solid blue line) is from Riva et al. (2019). Note that in case these PMF factors are internally mixed with other components, the predicted viscosity would not represent real ambient complex organic mixtures.

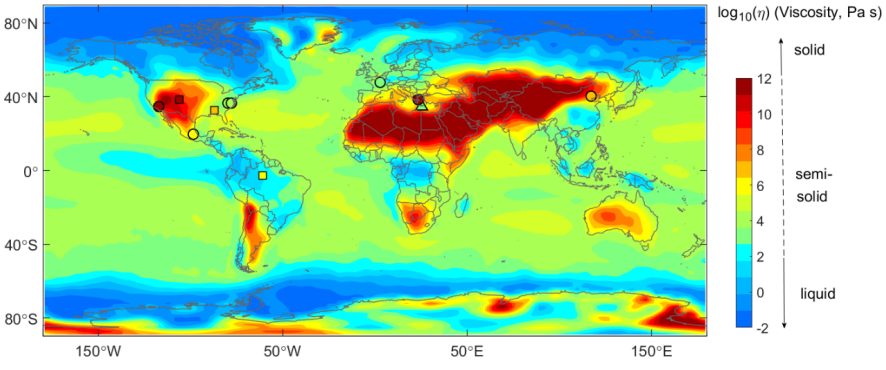

Figure 8. Comparison of global distributions of annual averages of SOA viscosity at the surface simulated by a chemical transport model (Shiraiwa et al., 2017) with the viscosity predicted by measured volatility distributions at 11 global sites as indicated with markers (triangle, circle and square represent remote, urban and forested sites, respectively, Table S2).

https://doi.org/10.5194/acp-2019-1132
Preprint. Discussion started: 6 January 2020

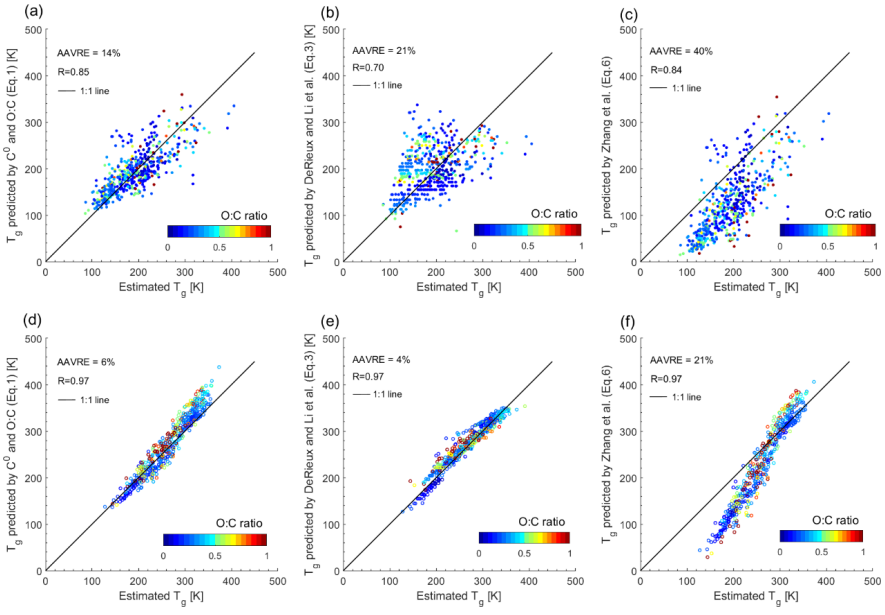

Figure A1. Predicted T_g for CHO compounds by (a) C^0 and O:C (Eq. 1), (b) elemental composition (Eq. 3), and (c) the parameterization (Eq. 6) in Zhang et al. (2019) plotted against estimated T_g. T_m and C^0 in (a) – (c) are measured; T_m and C^0 in (d) – (f) are estimated by the EPI Suite and the EVAPORATION model, respectively (see Supplement). Estimated T_g is then calculated from T_m applying the Boyer-Kauzmann rule. The markers are color-coded by the atomic O:C ratio. The solid line shows the 1:1 line. The correlation coefficient (R) and the average absolute value of the relative error (AAVRE) are shown.